

(*c* 1.10, MeOH);  $^1\text{H NMR}$  ( $\text{CD}_3\text{OD}$ )  $\delta$  3.38 (dd, 1H,  $J_{3-4}=J_{4-5}=9.4$  Hz, H-4), 3.53 (dd, 1H,  $J_{1-2}=3.6$  Hz,  $J_{2-3}=10.0$  Hz, H-2), 3.60 (ddd, 1H,  $J_{4-5}=9.4$  Hz,  $J_{5-6a}=5.0$  Hz,  $J_{5-6b}=2.4$  Hz, H-5), 3.66 (dd, 1H,  $J_{5-6a}=5.0$  Hz,  $J_{6a-6b}=11.8$  Hz, H-6a), 3.72 (dd, 1H,  $J_{5-6b}=2.4$  Hz,  $J_{6a-6b}=12.0$  Hz, H-6b), 3.80 (dd, 1H,  $J_{2-3}=J_{3-4}=9.4$  Hz, H-3), 5.39 (d, 1H,  $J=3.6$  Hz, H-1), 6.99 (d, 2H,  $J=9.2$  Hz,  $-\text{OC}_6\text{H}_4\text{NH}-$ ), 7.05 (d, 2H,  $J=9.2$  Hz,  $-\text{OC}_6\text{H}_4\text{NH}-$ ), 7.79 (d, 2H,  $J=8.4$  Hz,  $-\text{SO}_2\text{C}_6\text{H}_4\text{CF}_3$ ), 7.87 (d, 2H,  $J=8.4$  Hz,  $-\text{SO}_2\text{C}_6\text{H}_4\text{CF}_3$ ), MS: 478 (M-H) $^-$ .

**4-(4-Methylphenylsulfonylamino)phenyl  $\alpha$ -D-glucopyranoside (10).** According to method E, compound 10 was prepared from 20 (0.64 g, 1.1 mmol). The product was purified by column chromatography on silica gel (5:1  $\text{CH}_2\text{Cl}_2$ -MeOH) to afford a quantitative yield (0.50 g) of 10:  $[\alpha]_D^{+13.0}$  (*c* 1.98, MeOH);  $^1\text{H NMR}$  ( $\text{CD}_3\text{OD}$ )  $\delta$  2.37 (s, 3H,  $-\text{CH}_3$ ), 3.39 (dd, 1H,  $J_{3-4}=9.0$  Hz,  $J_{4-5}=9.8$  Hz, H-4), 3.53 (dd, 1H,  $J_{1-2}=3.6$  Hz,  $J_{2-3}=9.6$  Hz, H-2), 3.60 (ddd, 1H,  $J_{4-5}=9.8$  Hz,  $J_{5-6a}=5.2$  Hz,  $J_{5-6b}=2.4$  Hz, H-5), 3.66 (dd, 1H,  $J_{5-6a}=5.2$  Hz,  $J_{6a-6b}=12.0$  Hz, H-6a), 3.72 (dd, 1H,  $J_{5-6b}=2.4$  Hz,  $J_{6a-6b}=12.0$  Hz, H-6b), 3.80 (dd, 1H,  $J_{2-3}=J_{3-4}=9.2$  Hz, H-3), 5.37 (d, 1H,  $J=3.6$  Hz, H-1), 6.97 (d, 2H,  $J=9.6$  Hz,  $-\text{OC}_6\text{H}_4\text{NH}-$ ), 7.02 (d, 2H,  $J=9.2$  Hz,  $-\text{OC}_6\text{H}_4\text{NH}-$ ), 7.26 (d, 2H,  $J=8.4$  Hz,  $-\text{SO}_2\text{C}_6\text{H}_4\text{CH}_3$ ), 7.57 (d, 2H,  $J=8.4$  Hz,  $-\text{SO}_2\text{C}_6\text{H}_4\text{CH}_3$ ), MS: 424 (M-H) $^-$ .

**4-(4-*tert*-Butylphenylsulfonylamino)phenyl  $\alpha$ -D-glucopyranoside (11).** According to method E, compound 11 was prepared from 21 (0.55 g, 0.9 mmol). The product was purified by column chromatography on silica gel (5:1  $\text{CH}_2\text{Cl}_2$ -MeOH) to afford 0.40 g (99.7%) of 7:  $[\alpha]_D^{+11.8}$  (*c* 1.47, MeOH);  $^1\text{H NMR}$  ( $\text{CD}_3\text{OD}$ )  $\delta$  1.31 (s, 9H,  $-\text{C}(\text{CH}_3)_3$ ), 3.39 (dd, 1H,  $J_{3-4}=9.0$  Hz,  $J_{4-5}=9.8$  Hz, H-4), 3.53 (dd, 1H,  $J_{1-2}=3.6$  Hz,  $J_{2-3}=10.0$  Hz, H-2), 3.60 (ddd, 1H,  $J_{4-5}=9.8$  Hz,  $J_{5-6a}=4.8$  Hz,  $J_{5-6b}=2.4$  Hz, H-5), 3.66 (dd, 1H,  $J_{5-6a}=4.8$  Hz,  $J_{6a-6b}=12.0$  Hz, H-6a), 3.72 (dd, 1H,  $J_{5-6b}=2.4$  Hz,  $J_{6a-6b}=12.0$  Hz, H-6b), 3.80 (dd, 1H,  $J_{2-3}=J_{3-4}=9.4$  Hz, H-3), 5.37 (d, 1H,  $J=3.6$  Hz, H-1), 6.99 (d, 2H,  $J=9.2$  Hz,  $-\text{OC}_6\text{H}_4\text{NH}-$ ), 7.03 (d, 2H,  $J=9.6$  Hz,  $-\text{OC}_6\text{H}_4\text{NH}-$ ), 7.50 (d, 2H,  $J=8.4$  Hz,  $-\text{SO}_2\text{C}_6\text{H}_4\text{C}(\text{CH}_3)_3$ ), 7.62 (d, 2H,  $J=8.8$  Hz,  $-\text{SO}_2\text{C}_6\text{H}_4\text{C}(\text{CH}_3)_3$ ), MS: 466 (M-H) $^-$ .

**4-(2-Naphthalenophenylsulfonylamino)phenyl  $\alpha$ -D-glu-**

**copyranoside (12).** According to method E, compound 12 was prepared from 22 (0.53 g, 0.9 mmol). The product was recrystallized from hot EtOH to afford a quantitative yield 0.40 g of 12:  $[\alpha]_D^{+12.4}$  (*c* 1.24, MeOH);  $^1\text{H NMR}$  ( $\text{CD}_3\text{OD}$ )  $\delta$  3.37 (dd, 1H,  $J_{3-4}=8.8$  Hz,  $J_{4-5}=9.6$  Hz, H-4), 3.50 (dd, 1H,  $J_{1-2}=3.6$  Hz,  $J_{2-3}=10.0$  Hz, H-2), 3.56 (ddd, 1H,  $J_{4-5}=9.6$  Hz,  $J_{5-6a}=4.6$  Hz,  $J_{5-6b}=2.4$  Hz, H-5), 3.63 (dd, 1H,  $J_{5-6a}=4.6$  Hz,  $J_{6a-6b}=11.8$  Hz, H-6a), 3.67 (dd, 1H,  $J_{5-6b}=2.4$  Hz,  $J_{6a-6b}=11.8$  Hz, H-6b), 3.77 (dd, 1H,  $J_{2-3}=J_{3-4}=9.2$  Hz, H-3), 5.33 (d, 1H,  $J=3.6$  Hz, H-1), 7.00 (s, 4H,  $-\text{OC}_6\text{H}_4\text{NH}-$ ), 7.56–7.72, 7.91–7.96, 8.23 (m, 7H,  $-\text{SO}_2\text{C}_{10}\text{H}_7$ ), MS: 460 (M-H) $^-$ .

**Biological assays.** The  $\alpha$ -glucosidase inhibition assays were performed using *p*-nitrophenyl  $\alpha$ -D-glucopyranoside (Aldrich) as a substrate and were assayed using previously reported methods.<sup>13</sup> The DNA breakage activity was investigated using previously reported methods.<sup>16-18</sup> Inhibition assays at the cellular level were performed by previously reported methods.<sup>11</sup>

## RESULTS AND DISCUSSION

### Synthesis of sulfonate and sulfonamide derivatives.

The synthesis of the sulfonate derivatives 1–6 that were used in the present study is presented in Fig. 3.  $\alpha$ -Arbutin 13 was used as a starting material for the synthesis of compounds 1–6. Compound 13 was sulfonated with 4-nitrobenzenesulfonyl chloride, 4-chlorobenzenesulfonyl chloride, 4-trifluoromethylbenzenesulfonyl chloride, 4-methylbenzenesulfonyl chloride, 4-*t*-butylbenzenesulfonyl chloride, and 2-naphthalenesulfonyl chloride in acetone to give compounds 1–6, respectively.

The synthesis of the sulfonamide derivatives 7–12 that were used in the present study is presented in Fig. 4. *p*-Nitrophenyl  $\alpha$ -D-glucopyranoside 14 was used as a starting material for the synthesis of compounds 7–12. Compound 14 was acetylated with acetic anhydride in pyridine to give per-acetylated glucopyranoside 15. Compound 15 was hydrogenated under  $\text{H}_2$  with 20% palladium hydroxide on carbon to give the free-base 16. Compound 16 was sulfonated with 4-nitrobenzenesulfonyl chloride, 4-chloro-

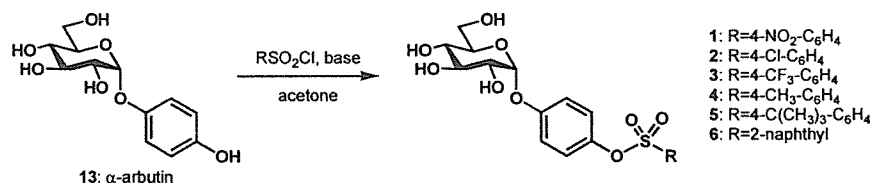
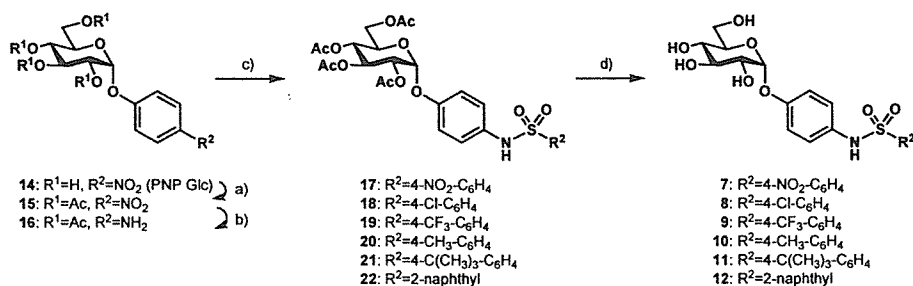


Fig. 3. Synthesis of compounds 1–6.



a)  $\text{Ac}_2\text{O}$ ,  $\text{C}_5\text{H}_5\text{N}$ , b)  $\text{Pd}(\text{OH})_2/\text{C}$ , EtOH, c)  $\text{R}^2\text{SO}_2\text{Cl}$ ,  $\text{C}_5\text{H}_5\text{N}$ , d)  $\text{NEt}_3$ ,  $\text{H}_2\text{O}$ , MeOH

Fig. 4. Synthesis of compounds 7–12.

benzenesulfonyl chloride, 4-trifluoromethylbenzenesulfonyl chloride, 4-methylbenzenesulfonyl chloride, 4-*t*-butylbenzenesulfonyl chloride, and 2-naphthalenesulfonyl chloride in pyridine to give 17–22 in good yields, respectively. Treatment of the resulting sulfonamides 17–22 with base gave compounds 7–12 in good yields, respectively. To the best of our knowledge, there have been no previous reports on the synthesis of compounds 1–6, 8–9 or 11. Data for NMR and MS spectra and optical rotation of all compounds 1–12 have not been reported.

#### Inhibition of $\alpha$ -glucosidases.

Inhibition studies on compounds 1–12 towards *Saccharomyces cerevisiae*, *Bacillus stearothermophilus* and rice  $\alpha$ -glucosidases, and the results are listed in Table 1. Compounds 6 and 12, with a terminal 2-naphthyl group, indicated inhibitions of  $\alpha$ -glucosidases from *S. cerevisiae* ( $IC_{50}$ =51.7  $\mu$ M and  $IC_{50}$ =74.1  $\mu$ M) and *B. stearothermophilus* ( $IC_{50}$ =60.1  $\mu$ M and  $IC_{50}$ =89.1  $\mu$ M). Compounds 1–5 and 7–11 showed no significant inhibitory properties for *S. cerevisiae* or *B. stearothermophilus*  $\alpha$ -glucosidases. No compounds inhibited rice  $\alpha$ -glucosidase. Additionally, all  $\alpha$ -glucosidases hydrolyzed compounds 1–12. These results indicated that compounds 1–12 have properties of both substrate and inhibitor against *S. cerevisiae*  $\alpha$ -glucosidase. Compounds 1–5 were substrate for *B. stearothermophilus* enzyme. However, compounds 6–12 were substrate and inhibitor for *B. stearothermophilus* enzyme. All compounds were substrate for rice enzyme. From these results if *p*-benzoquinone or *p*-benzoquinone imine are released during the liberation of the aglycon of compounds 1–12, the huge differences in enzyme inhibitory activity among three kinds of enzymes will not result. This speculation is

**Table 1.** Inhibitory activities of compounds 1–12 against  $\alpha$ -glucosidases.

Compound	$IC_{50}$ ( $\mu$ M)		
	<i>S. cerevisiae</i>	<i>B. stearothermophilus</i>	Rice
1	499	>500	>500
2	437	>500	>500
3	407	>500	>500
4	499	>500	>500
5	391	>500	>500
6	51.7	60.1	>500
7	239	218	>500
8	200	254	>500
9	146	244	>500
10	231	325	>500
11	136	237	>500
12	74.1	89.1	>500

The *S. cerevisiae* and *B. stearothermophilus*  $\alpha$ -glucosidase inhibition assays were performed by using 1 mM PNP Glc as substrate. The assay conditions were potassium phosphate buffer (pH 7.0) at 37°C, 20 min. The rice  $\alpha$ -glucosidase inhibition assay was performed by using 1 mM PNP Glc as substrate. The assay conditions were sodium acetate buffer (pH 4.0) at 37°C, 60 min. All  $\alpha$ -glucosidases hydrolyzed compounds 1–12.

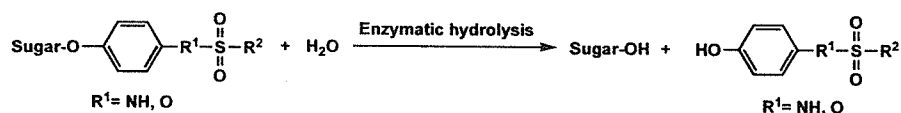


**Fig. 5.** Schematic diagram of enzymatic liberation of phenol derivatives.

in conflict with those expected from the theory shown in Fig. 2. Therefore, the enzymatic hydrolysis reaction of compound 4 in the presence of *S. cerevisiae*  $\alpha$ -glucosidase was analyzed using the LC/MS system as a model case. It was found that the major product of the hydrolysis reaction was aphenol compound corresponding to the aglycon moiety of compound 4 (data not shown).  $\alpha$ -Glucosidase inhibition of compounds 1–12 was considered to be due to the enzymatic formation of phenol derivatives from compounds 1–12, illustrated in Fig. 5, and/or compounds 1–12 themselves.

#### DNA Cleavage activities.

Fukuhara *et al.* have reported that a phenol compound, resveratrol, induced Cu(II)-dependent DNA-strand scission under neutral conditions.<sup>17)</sup> This DNA cleavage process occurs in the presence of Cu(II) and O<sub>2</sub>. The ability of compounds 1–12 to induce DNA cleaving activity was examined using pBR322, a supercoiled, covalently closed circular DNA (Form I), and analyzed by agarose gel electrophoresis (Table 2).  $\alpha$ -Glucosidase-triggered radical-mediated DNA breakage was very effectively observed for sulfonamide derivatives 7–12. Consistent with the fact that Cu(II) and enzyme are required for potent DNA cleaving activity of compounds 7–12, these compounds induced DNA cleavage only when the reaction was carried out in the presence of Cu(II) and enzyme; in the absence of Cu(II) and enzyme, no DNA cleavage was observed. On the other hand, sulfonate derivatives 1–6 caused only slight damage under the same conditions. The decrease in the DNA cleaving ability of compounds 1–6 compared to that of compounds 7–12 also indicated the importance of the sulfonamide structure, which might be

**Table 2.** Enzyme-triggered DNA-cleaving activities of compounds 1–12.

Compound	CuCl <sub>2</sub> NADH Enzyme	Residual ratio of Form I plasmid (%)				
		+	+	-	-	+
		+	-	+	-	+
1		86	100	100	100	100
2		87	100	100	100	100
3		91	72	100	100	100
4		93	100	100	100	100
5		85	100	100	100	100
6		76	64	100	100	100
7		<1	<1	100	100	100
8		<1	<1	100	100	100
9		<1	23	100	100	100
10		<1	17	100	100	100
11		<1	6	100	100	100
12		<1	22	100	100	100

Analysis of DNA strand breaks generated in pBR322DNA with compounds 1–12. Assays were performed by using 1 mM of compound, 100  $\mu$ M CuCl<sub>2</sub>, 500  $\mu$ M NADH, and *S. cerevisiae*  $\alpha$ -glucosidase. The assay conditions were sodium phosphate buffer (pH 7.0) containing pBR322DNA at 37°C, for 20 h.

effective not only for DNA binding for the conformation of the overall structure but also for the stability of the phenoxy radical. No effect of DNA cleaving activity of compounds 1–12 was observed in spite of the presence of NADH. It would appear that the enzymatic liberation of quinone derivative shown in Fig. 2 does not occur, since quinone derivatives showed DNA cleaving activity in the presence of NADH.<sup>15</sup> These findings can be explained by the fact that enzymatic liberation of the aglycon from compounds 1–12 was followed by the ejection of phenol derivatives, shown in Fig. 5.

#### Cellular level assays.

Compounds 1–12 were assayed with regard to their ability to inhibit ER glucosidase at the cellular level. Vesicular stomatitis virus glycoprotein (VSV G) was prepared from VSV-infected and probe-treated baby hamster kidney (BHK) cells. Analyses of the *N*-glycan structure of obtained VSV G using endo H, which is known to have hydrolytic activity against high-mannose type *N*-glycan, failed to confirm that these compounds inhibited ER glucosidases (data not shown).

We have shown that dual functional small molecules having both the  $\alpha$ -glucosidase inhibitory activity and DNA breakage activity at the enzyme level can be designed, using our mechanism-based approach. We plan in the near future to study the structure-activity relationship and to extend the same strategies to more complicated cellular systems. We think that ER-targeted small molecule apoptosis inducers are necessary for the development of new and potent antitumor agents.

This research was partly supported by the Ministry of Education, Science, Sports and Culture Grant-in-Aid for Young Scientists (B) (No. 17790097) and Health and Labour Sciences Research Grants for Research on HIV/AIDS to W.H. from the Ministry of Health, Labour and Welfare, Japan. We thank Ezaki Glico Co., Ltd., for the gift of  $\alpha$ -arbutin.

#### REFERENCES

- 1) U. Fischer and K. Schulze-Osthoff: Apoptosis-based therapies and drug targets. *Cell Death Differ.*, **12**, 942–961 (2005).
- 2) Y. Ma and L.M. Hendershot: The unfolding tale of the unfolded protein response. *Cell*, **107**, 827–830 (2001).
- 3) M. Schroder and R.J. Kaufman: ER stress and the unfolded protein response. *Mutat. Res.*, **569**, 29–63 (2005).
- 4) C.R. Bertozzi and L.L. Kiessling: Chemical glycobiology. *Science*, **291**, 2357–2364 (2001).
- 5) S.W. Fesik: Promoting apoptosis as a strategy for cancer drug discovery. *Nat. Rev. Cancer*, **5**, 876–885 (2005).
- 6) T. Nishio, Y. Miyake, H. Tsujii, W. Hakamata, K. Kadokura and T. Oku: Hydrolytic activity of  $\alpha$ -mannosidase against deoxy derivatives of *p*-nitrophenyl  $\alpha$ -D-mannopyranoside. *Biosci. Biotech. Biochem.*, **60**, 2038–2042 (1996).
- 7) W. Hakamata, T. Nishio and T. Oku: Synthesis of *p*-nitrophenyl 3- and 6-deoxy- $\alpha$ -D-glucopyranosides and their specificity to rice  $\alpha$ -glucosidase. *J. Appl. Glycosci.*, **46**, 459–463 (1999).
- 8) W. Hakamata, T. Nishio and T. Oku: Hydrolytic activity of  $\alpha$ -galactosidase against deoxy derivatives of *p*-nitrophenyl  $\alpha$ -D-galactopyranoside. *Carbohydr. Res.*, **324**, 107–115 (2000).
- 9) W. Hakamata, T. Nishio, R. Sato, T. Mochizuki, K. Tsuchiya, M. Yasuda and T. Oku: Synthesis of monomethyl derivatives of *p*-nitrophenyl  $\alpha$ -D-glucopyranoside, galactopyranoside and mannopyranoside and their hydrolytic properties against  $\alpha$ -glucosidase. *J. Carbohydr. Chem.*, **19**, 359–377 (2000).
- 10) T. Nishio, W. Hakamata, A. Kimura, S. Chiba, A. Takatsuki, R. Kawachi and T. Oku: Glycon specificity profiling of  $\alpha$ -glucosidases using monodeoxy and mono-*O*-methyl derivatives

- of *p*-nitrophenyl  $\alpha$ -D-glucopyranoside. *Carbohydr. Res.*, **337**, 629–634 (2002).
- 11) W. Hakamata, M. Muroi, T. Nishio, T. Oku and A. Takatsuki: Recognition properties of processing  $\alpha$ -glucosidase I and  $\alpha$ -glucosidase II. *J. Carbohydr. Chem.*, **23**, 27–39 (2004).
  - 12) T. Nishio, W. Hakamata, M. Ogawa, K. Nakajima, Y. Matsuishi, R. Kawachi and T. Oku: Investigations of useful  $\alpha$ -glucosidase for the enzymatic synthesis of rare sugar oligosaccharides. *J. Appl. Glycosci.*, **52**, 153–160 (2005).
  - 13) W. Hakamata, M. Muroi, K. Kadokura, T. Nishio, T. Oku, A. Kimura, S. Chiba and A. Takatsuki: Aglycon specificity profiling of  $\alpha$ -glucosidases using synthetic probes. *Bioorg. Med. Chem. Lett.*, **15**, 1489–1492 (2005).
  - 14) W. Hakamata, I. Nakanishi, Y. Masuda, T. Shimizu, H. Higuchi, Y. Nakamura, T. Oku, S. Saito, S. Urano, T. Ozawa, N. Ikota, N. Miyata, H. Okuda and K. Fukuhara: Planar catechin analogues with alkyl aide chain, a potent antioxidant and  $\alpha$ -glucosidase inhibitor. *J. Am. Chem. Soc.*, **128**, 6524–6525 (2006).
  - 15) J.C. Briggs, A.H. Haines and R.J.K. Taylor: 4-(Sulfonylamino) phenyl  $\alpha$ -D-glucopyranoside as competitive inhibitor of yeast  $\alpha$ -glucosidase. *J. Chem. Soc. Chem. Commun.*, **18**, 1410–1411 (1993).
  - 16) K. Fukuhara, Y. Naito, Y. Sato, I. Nakanishi and N. Miyata: Generation of oxygen radicals and DNA-cleaving ability in quinone/NADH system. *Magnet. Reson. Med.*, **13**, 139–142 (2002).
  - 17) K. Fukuhara and N. Miyata: Resveratrol as a new type of DNA-cleaving agent. *Bioorg. Med. Chem. Lett.*, **8**, 3187–3192 (1998).
  - 18) K. Fukuhara, M. Nagakawa, I. Nakanishi, K. Ohkubo, K. Imai, S. Urano, S. Fukuzumi, T. Ozawa, N. Ikota, M. Mochizuki, N. Miyata and H. Okuda: Structural basis for DNA-cleaving activity of resveratrol in the presence of Cu(II). *Bioorg. Med. Chem.*, **14**, 1437–1473 (2006).

#### DNA 切断活性を有する $\alpha$ -グルコシダーゼ阻害剤の設計と合成

袴田 航<sup>1</sup>, 山本恵美子<sup>1,2</sup>, 室井 誠<sup>3</sup>, 望月正隆<sup>2</sup>

栗原正明<sup>1</sup>, 奥田晴宏<sup>1</sup>, 福原 潔<sup>1</sup>

<sup>1</sup> 国立医薬品食品衛生研究所有機化学部

(158-8501 東京都世田谷区上用賀 1-18-1)

<sup>2</sup> 共立薬科大学薬学部

(105-8512 東京都港区芝公園 1-5-30)

<sup>3</sup> 理化学研究所長田抗生物質研究室

(351-0198 和光市広沢 2-1)

グルコース飢餓、ウイルス感染、低酸素状態などの小胞体ストレスは小胞体に高次構造異常タンパク質を蓄積させる。細胞は分子シャペロンを転写レベルで誘導する unfolded protein response (UPR) を誘起するなどして小胞体ストレスに抵抗するが、強い小胞体ストレスは細胞をアポトーシスへと誘導する。よって小胞体ストレスに起因するアポトーシスをがん細胞で誘導する化合物は抗がん剤となりうる。現在、新規な抗腫瘍薬の一つとして、がん細胞におけるアポトーシス誘導を標的とした抗腫瘍薬の開発が行われている。そこで我々は、*N*-結合型糖鎖プロセッシング酵素を阻害することにより小胞体に高次構造異常タンパク質を蓄積させ、それによる小胞体ストレスによって誘起される UPR を阻害することによりアポトーシスを誘導する化合物(小分子アポトーシス誘導化合物)としてスルホンエステル誘導体(1–6)とスルホンアミド誘導体(7–12)を設計し(Fig. 1)合成を行った(Fig. 3–4)。合成した化合物(1–12)の  $\alpha$ -グルコシダーゼ阻害活性(Table 1)と DNA 切断活性(Table 2)について検討を行った。更に、細胞レベルでの *N*-結合型糖鎖プロセッシング酵素阻害活性についても検討した。その結果、ナフチル基を有する化合物 6 と 12 が、*S. cerevisiae* 由来  $\alpha$ -グルコシダーゼに対し IC<sub>50</sub>=51.7  $\mu$ M と 74.1  $\mu$ M、*B. stearothermophilus* 由来  $\alpha$ -グルコシダーゼに対し IC<sub>50</sub>=60.1  $\mu$ M と 89.1  $\mu$ M の阻害活性を示し、化合物 12 が最も強く DNA 切断活性を示した。しかし、すべての化合物が細胞レベルにおいて、酵素阻害活性を示さなかった。以上、酵素レベルにおいて  $\alpha$ -グルコシダーゼ阻害活性と DNA 切断活性を有する小分子を見いだした。今後は、細胞レベルにおいても有効な化合物設計を行う予定である。

## Planar Catechin Analogues with Alkyl Side Chains: A Potent Antioxidant and an $\alpha$ -Glucosidase Inhibitor

Wataru Hakamata,<sup>†</sup> Ikuo Nakanishi,<sup>‡,§</sup> Yu Masuda,<sup>||</sup> Takehiko Shimizu,<sup>⊥</sup> Hajime Higuchi,<sup>⊥</sup> Yuriko Nakamura,<sup>#</sup> Shinichi Saito,<sup>#</sup> Shiro Urano,<sup>⊥</sup> Tadatake Oku,<sup>||</sup> Toshihiko Ozawa,<sup>‡</sup> Nobuo Ikota,<sup>‡</sup> Naoki Miyata,<sup>◇</sup> Haruhiro Okuda,<sup>†</sup> and Kiyoshi Fukuhara<sup>\*†</sup>

*Division of Organic Chemistry, National Institute of Health Sciences, Setagaya-ku, Tokyo 158-8501, Japan, Redox Regulation Research Group, Research Center for Radiation Safety, National Institute of Radiological Sciences, Inage-ku, Chiba 263-8555, Japan, Graduate School of Engineering, Osaka University, SORST, Japan Science and Technology Agency, Suita, Osaka 565-0871, Japan, College of Bioresource Sciences, Nihon University, Fujisawa, Kanagawa 1866, Japan, Department of Applied Chemistry, Shibaura Institute of Technology, Minato-ku, Tokyo 108-8548, Japan, Faculty of Science, Tokyo University of Science, Shinjuku-ku, Tokyo 162-8601, Japan, and Graduate School of Pharmaceutical Sciences, Nagoya City University, Mizuho-ku, Nagoya, Aichi 467-8603, Japan*

Received November 15, 2005; E-mail: fukuhara@nihs.go.jp

As mitochondrial oxidative damage<sup>1</sup> or oxidative modification of low-density lipoprotein (LDL)<sup>2</sup> contribute significantly to a range of degenerative diseases and further production of reactive oxygen species (ROS), it might be advantageous to develop lipophilic antioxidants which would be able to suppress mitochondrial ROS production or LDL oxidation due to their affinity to lipid particles or membrane. Recently, we synthesized planar catechin analogue (PC1), in which the catechol and chroman structure in (+)-catechin are constrained to be planar, by the reaction of (+)-catechin with acetone in the presence of BF<sub>3</sub>·Et<sub>2</sub>O.<sup>3,4</sup> The rate of hydrogen transfer from PC1 to galvinoxyl radical (G•), a stable oxygen-centered radical, is about 5-fold faster than that of hydrogen transfer from the native (+)-catechin to G•. PC1 also shows an enhanced protective effect against oxidative DNA damage induced by the Fenton reaction without the pro-oxidant effect, which is usually observed in the case of (+)-catechin. We also have found that PC1, as well as stilbene resveratrol<sup>5</sup> which is a typical cancer chemopreventive agent present in grapes, inhibits cell growth through induction of apoptosis in cancer cell lines (data not shown). Therefore, we envisioned that a conformationally constrained planar catechin might be valuable in the development of a new type of clinically useful antioxidant, if the hydrophobicity of PC1 could be controlled so as to fine-tune its membrane binding and penetration into the phospholipid bilayer. Here, we describe a synthetic method for planar catechin analogues (PCn), the lipophilicity of which was controlled by changing the length of the alkyl chains. Also described are their remarkable antioxidative potencies and  $\alpha$ -glucosidase inhibitory activities.

The synthesis of PCn was carried out by reacting catechin with various ketones having alkyl chains of different lengths. However, the previously reported method for the synthesis of PC1<sup>3</sup> is inapplicable to other PCn synthesis. Because the original reaction is carried out in a solution of acetone, the synthesis of PCn is limited to using the corresponding ketone as a solvent. Therefore, it was necessary to improve the synthetic method of PC1 to be able to introduce various types of ketones into the catechin structure using a synthetic scheme applicable for any PCn production. We attempted to optimize the reaction using a combination of various acids and solvents, and finally, it was shown that the reaction using

silyl Lewis acids such as TMSOTf, TESOTf, or TBSOTf gave the desired products in high yields. Typically, (+)-catechin and 1.2 equiv of ketone in THF was treated with 1.2 equiv of TMSOTf at -5 °C to form the desired PCn. This reaction was used to provide a series of PC1  $\approx$  PC6, 44–76% yield (Scheme 1), with slightly different lipophilicity.

PCn were evaluated for their radical scavenging activities against DPPH (2,2-di(4-tert-octylphenyl)-1-picrylhydrazyl) radical and AAPH (2,2'-azobis(2-amidinopropane) dihydrochloride)-derived peroxy radical (Scheme 2). The hydrogen abstraction of PCn by DPPH radical in deaerated acetonitrile solution was monitored using the decrease of the visible absorption band at 543 nm due to DPPH radical that obeyed pseudo-first-order kinetics. The second-order rate constant ( $k_{HT}$ ) for hydrogen abstraction of PCn by DPPH radical was then determined (Table 1). Similar to what was found with hydrogen abstraction by galvinoxyl radical,<sup>3</sup> the  $k_{HT}$  value (533 M<sup>-1</sup> s<sup>-1</sup>) of PC1 is significantly larger than that of (+)-catechin (305 M<sup>-1</sup> s<sup>-1</sup>), indicating that the radical-scavenging activity of catechin using DPPH radical increased due to constraining the (+)-catechin in a planar configuration. In addition, it was found that the larger the number of carbon atoms there were in the alkyl chains, the greater the DPPH radical scavenging rates became, with the  $k_{HT}$  value of PCn plateauing at  $n = 4$ . The radical scavenging ability of PCn with longer side chains might be attributed to the -I effect of the side chain that stabilizes the cation radical formed after electron transfer from PCn to DPPH. The radical scavenging activities of PCn in aqueous solution were investigated using AAPH as a source of free radicals in phosphate buffer (Table 1). AAPH-derived peroxy radicals react with luminol to generate prolonged luminescence,<sup>6</sup> and the antioxidative activities of PCn were determined using the concentration of PCn where the luminescence is reduced to 50%. As a result, the antioxidative activity of planar catechin in phosphate buffer was again stronger than that of catechin as well as its antioxidative activity in acetonitrile. The alkyl side chains also affect the antioxidative activity; an increase ( $n = 1-3$ ) in the length of the alkyl chains tends to increase the antioxidative activity, with PC3 showing the strongest antioxidative effect. However, further increase ( $n = 4-6$ ) in the length of the side chain seems to weaken the antioxidative effects, which is consistent with the suggestion that longer alkyl side chains result in the formation of amphiphilic micelles in aqueous solvent.

For the evaluation of lipophilic PCn as antioxidants against biomolecular injury caused by ROS, the protecting effect of PCn on oxidative DNA damage induced by the Fenton reaction was

<sup>†</sup> National Institute of Health Sciences, Japan.

<sup>‡</sup> National Institute of Radiological Sciences, Japan.

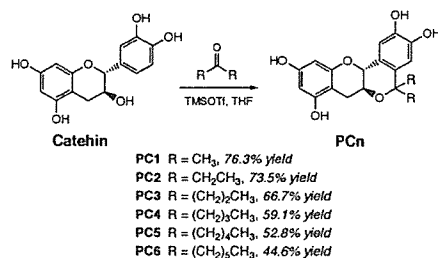
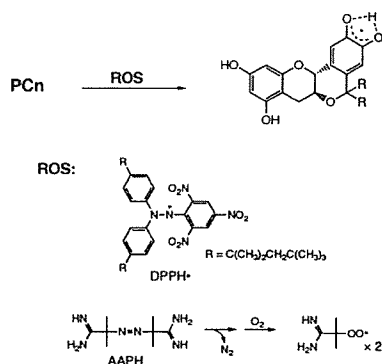
<sup>§</sup> Osaka University, SORST, Japan Science and Technology Agency.

<sup>||</sup> Nihon University.

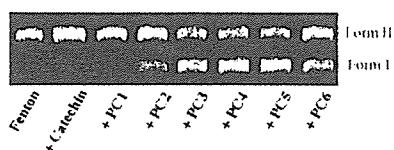
<sup>⊥</sup> Shibaura Institute of Technology.

<sup>#</sup> Tokyo University of Science.

<sup>◇</sup> Nagoya City University.

**Scheme 1.** Chemical Structure and Synthesis of PCn**Scheme 2.** Radical Scavenging Reaction of PCn against DPPH• and AAPH**Table 1.** Antioxidant Profile of Catechin and PCn Determined Using a DPPH and AAPH Scavenging Assay

compd	DPPH• $k_{\text{H}}$ (M <sup>-1</sup> s <sup>-1</sup> )	AAPH IC <sub>50</sub> (nM)
catechin	305	292
PC1	533	220
PC2	622	175
PC3	686	98
PC4	725	147
PC5	756	625
PC6	759	1700

**Figure 1.** Effects of catechin and PCn on DNA breakage induced by the Fenton reaction (Fe<sup>3+</sup>/H<sub>2</sub>O<sub>2</sub>). Assays were performed in 100 mM phosphate buffer, pH 7.0 containing 45 μM pBR322DNA, 10 mM H<sub>2</sub>O<sub>2</sub>, 100 μM FeCl<sub>3</sub>, and 1 mM individual PCn for 1 h at 37 °C.

determined. Although PC1 showed an excellent protecting effect against oxidative DNA scission compared with catechin,<sup>3</sup> the antioxidative activity of the series of PCn was evaluated under conditions in which the protecting effect of PC1 appears to be weak. As shown in Figure 1, DNA cleaving activity induced by the Fenton reaction did not increase in the presence of PCn, and with an increase in the length of alkyl chains, the protecting effect of PCn on the oxidative DNA damage was greatly increased. The strong antioxidative activity might be attributed to a combination of radical scavenging activity and lipophilicity that tends to increase the binding between PCn and DNA. A small decrease in the protecting effect of PC6 might be responsible for the diminishing radical scavenging ability under aqueous solution.

In addition to the antioxidative ability, (+)-catechin is known to be an inhibitor against α-glucosidase<sup>7</sup> that catalyzes the final

**Table 2.** Inhibitory Activities of Catechin and PCn against α-glucosidases

compd	<i>S. cerevisiae</i> IC <sub>50</sub> (μM)	<i>B. stearothermophilus</i> IC <sub>50</sub> (μM)
catechin	>500	>500
PC1	1.2	0.7
PC2	47.5	26.8
PC3	37.5	28.4
PC4	2.1	14.2
PC5	5.3	6.8
PC6	0.9	1.1

step in the digestive process of carbohydrates. Therefore, the inhibitory effects of PCn on α-glucosidase from *Saccharomyces cerevisiae* and *Bacillus stearothermophilus* were evaluated (Table 2). Surprisingly, in contrast to the relative weak inhibitory effect of (+)-catechin with IC<sub>50</sub> > 500 μM, PCn exhibited strong inhibitory effects with IC<sub>50</sub> = 0.7–47.5 μM against both enzymes, with PC1 (IC<sub>50</sub> = 1.2 μM for *S. cerevisiae* and 0.7 μM for *B. stearothermophilus*) and PC6 (IC<sub>50</sub> = 0.9 μM for *S. cerevisiae* and 1.1 μM for *B. stearothermophilus*) showing especially high inhibition concentrations. The strong inhibitory effect of PCn on α-glucosidase suggested that these planar catechin analogues may be used as a lead compounds for the development of antidiabetic therapeutics, similar to acarbose and voglibose which are known to reduce postprandial hyperglycemia primarily by interfering with the carbohydrate digesting enzymes and delaying glucose absorption.

In summary, a practical method for the preparation of planar catechin analogues with various alkyl side chain lengths is described as well as the remarkable properties of these compounds as potent antioxidants and α-glucosidase inhibitors. In vivo studies to fully exploit these potential benefits of PCn are currently under way, and the results will be published in due time.

**Acknowledgment.** This work was supported partly by a Grant from the Ministry of Health, Labor and Welfare, and by a Grant-in-Aid for Research of Health Sciences focusing on Drug Innovation (KH51058) from the Japan Health Sciences Foundation, partly by Grant-in-Aids for Scientific Research (B) (No. 17390033) and for Young Scientist (B) (No. 17790044) from the Ministry of Education, Culture, Sports, Science and Technology, Japan.

**Note Added after ASAP Publication.** After this paper was published ASAP on May 3, 2006, Table 2 was corrected to show the *S. cerevisiae* IC<sub>50</sub> value of 1.2 μM for PC1.

**Supporting Information Available:** Experimental details. This material is available free of charge via the Internet at <http://pubs.acs.org>.

## References

- (1) (a) Raha, S.; Robinson, B. H. *Am. J. Med. Genet.* 2001, 106, 62. (b) Kang, D.; Hamasaki, N. *Curr. Med. Chem.* 2005, 12, 429.
- (2) Tsimilas, S.; Witztum, J. L. In *Oxidative stress and vascular diseases*; Keane, J. F., Jr., Ed.; Kluwer: Boston, 2000; pp 49–74.
- (3) Fukuhara, K.; Nakanishi, I.; Kansui, H.; Sugiyama, E.; Kimura, M.; Shimada, T.; Urano, S.; Yamaguchi, K.; Miyata, N. *J. Am. Chem. Soc.* 2002, 124, 5952.
- (4) (a) Fukuhara, K.; Nakanishi, I.; Shimada, T.; Miyazaki, K.; Hakamata, W.; Urano, S.; Ikota, N.; Ozawa, T.; Okuda, H.; Miyata, N.; Fukuzumi, S. *Chem. Res. Toxicol.* 2003, 16, 81. (b) Nakanishi, I.; Ohkubo, K.; Miyazaki, K.; Hakamata, W.; Urano, S.; Ozawa, T.; Okuda, H.; Fukuzumi, S.; Ikota, N.; Fukuhara, K. *Chem. Res. Toxicol.* 2004, 17, 26.
- (5) Joe, A. K.; Liu, H.; Suzui, M.; Vural, M. E.; Xiao, D.; Weinstein, I. B. *Clin. Cancer Res.* 2002, 8, 893.
- (6) Krasowska, A.; Rosiak, D.; Szkapiak, K.; Oswiecimska, M.; Witek, S.; Lukaszewicz, M. *Cell. Mol. Biol. Lett.* 2001, 6, 71.
- (7) Matsui, T.; Yoshimoto, C.; Osajima, K.; Oki, T.; Osajima, Y. *Biosci. Biotechnol. Biochem.* 1996, 60, 2019.

JA057763C

## N-Linked Oligosaccharide Processing Enzymes as Molecular Targets for Drug Discovery

(Received December 1, 2005)

Wataru Hakamata,<sup>1,\*</sup> Makoto Muroi,<sup>2</sup> Toshiyuki Nishio,<sup>3</sup> Tadatake Oku,<sup>3</sup> Akira Takatsuki,<sup>4</sup>  
 Hiroyuki Osada,<sup>2</sup> Kiyoshi Fukuhara,<sup>1</sup> Haruhiro Okuda<sup>1</sup> and Masaaki Kurihara<sup>1</sup>

<sup>1</sup>*Division of Organic Chemistry, National Institute of Health Sciences (NIHS)*  
 (1-18-1, Kamiyoga, Setagaya-ku, Tokyo 158-8501, Japan)

<sup>2</sup>*Antibiotics Laboratory, The Institute of Physical and Chemical Research (RIKEN)*  
 (2-1, Hirosawa, Wako, Saitama 351-0198, Japan)

<sup>3</sup>*Department of Biological Chemistry, College of Bioresource Sciences, Nihon University*  
 (1866, Kameino, Fujisawa, Kanagawa 252-8510, Japan)

<sup>4</sup>*Department of Materials Chemistry, Faculty of Engineering, Hosei University*  
 (3-7-2, Kajino-cho, Koganei, Tokyo 184-8584, Japan)

**Abstract:** N-Linked oligosaccharide processing enzymes are key enzymes in the biosynthesis of N-linked oligosaccharides. These enzymes are a molecular target for inhibition by anti-viral agents that interfere with the formation of essential glycoproteins required in viral assembly, secretion and infectivity. We think that the molecular recognition of three kinds of glucosidases (family 13 and family 31  $\alpha$ -glucosidases and endoplasmic reticulum glucosidases) are different. Therefore, glycon and aglycon specificity profiling of glucosidases was an important approach for the research of glucosidase inhibitors. We carried out the profiling of glucosidases using small molecules as a probe. Moreover, we designed and synthesized three types of glucosidase inhibitors. These compounds were evaluated with regard to their ability to inhibit glucosidases *in vitro*, and were also tested in a cell culture system. We found some compounds having glucosidase inhibitory activity and anti-viral activity.

**Key words:**  $\alpha$ -glucosidase, ER glucosidase, inhibitor, anti-viral activity

$\alpha$ -Glucosidases (EC 3.2.1.20) are also exo-acting carbohydrases, catalyzing the release of  $\alpha$ -D-glucopyranose from the non-reducing ends of various substrates,<sup>1,2)</sup> and on the basis of amino acid sequence similarities,  $\alpha$ -glucosidases are classified into two families, family 13 and family 31.<sup>3,4)</sup> Endoplasmic reticulum (ER) glucosidases, glucosidase I (EC 3.2.1.106) and glucosidase II (EC 3.2.1.84), are key enzymes in the biosynthesis of asparagine-linked oligosaccharides that catalyze the first processing event after the transfer of Glc<sub>3</sub>Man<sub>9</sub>GlcNAc<sub>2</sub> to proteins. These enzymes are a target for inhibition by anti-viral agents that interfere with the formation of essential glycoproteins required in viral assembly, secretion and infectivity.<sup>5)</sup> Many papers reported that inhibitors of  $\alpha$ -glucosidases are potential therapeutics for the treatment of such diseases as viral diseases, cancer and diabetes.<sup>5,6)</sup> However, many screenings of  $\alpha$ -glucosidase inhibitors did not use enzymes from target tissues or organs. We think that the molecular recognitions of three kinds of glucosidases (family 13, family 31  $\alpha$ -glucosidases and ER glucosidases) are different. Therefore, the glycon and aglycon specificity profiling of glucosidases has been an important approach for the research of glucosidase inhibitors.

In this research, we first describe the glycon and aglycon specificity profiling of glucosidases using small molecules as probes. Next, compounds designed and synthe-

sized as glucosidase inhibitor candidates were evaluated with regard to their ability to inhibit three kinds of glucosidases. Finally, the glucosidase inhibitor candidates were tested for their anti-viral activities in a cell culture system.

### *Glycon specificity profiling of glucosidases using chemically modified substrates.*

Chemically modified substrates are effective methods in the study of substrate specificity profiling. We have applied this approach to family 13 and family 31  $\alpha$ -glucosidases,<sup>7-10)</sup> ER glucosidases,<sup>11,12)</sup>  $\alpha$ -galactosidases<sup>8,13)</sup> and  $\alpha$ -mannosidases<sup>3,14)</sup> using partially substituted monosaccharides. We used all of the monodeoxy analogs of *p*-nitrophenyl  $\alpha$ -D-glucopyranoside (PNP  $\alpha$ -Glc) 1–4 (Fig. 1) as chemically modified substrates for glycon specificity profiling. We investigated the hydrolytic activities of family 13 and family 31  $\alpha$ -glucosidases and ER glucosidase II of PNP  $\alpha$ -Glc and its deoxy derivatives 1–4, and checked the inhibitory activities of ER glucosidase I of PNP  $\alpha$ -Glc and probes 1–4, so that PNP  $\alpha$ -Glc was not a substrate for ER glucosidase I. These results are shown in Table 1.<sup>11,12)</sup> Clearly, of the four deoxy derivatives of PNP  $\alpha$ -Glc 1–4, family 31  $\alpha$ -glucosidases and ER glucosidase II hydrolyzed the 2-deoxy glucopyranoside (**1**); its activity with **1** appeared to be substantially higher than that with PNP  $\alpha$ -Glc. Kinetic studies of the hydrolysis of PNP  $\alpha$ -Glc, **1** and **2** were also carried out (Table 2).<sup>9,11)</sup> The  $V_{max}/K_m$  or  $k_{cat}/K_m$  values of family 31  $\alpha$ -glucosidases

\* Corresponding author (Tel. +81-3-3700-1141, Fax. +81-3-3707-6950, E-mail: hakamata@nihs.go.jp).

and ER glucosidase II for **1** was about twice as great as PNP  $\alpha$ -Glc, which indicated that probe **1** was a good substrate for the enzymes. These reaction velocities to probe **1** increased to 3–28 fold that of PNP  $\alpha$ -Glc. PNP Glc and probes **1–4** inhibited ER glucosidase I by 56.2, 71.7, 18.5, 22.2 and 32.3% at 5 mM, respectively. These results also indicated that ER glucosidase II might have properties similar to those found in family 31  $\alpha$ -glucosidases.

#### Aglycon specificity profiling and inhibition of glucosidases using heptitol derivatives.

For aglycon specificity profiling, we designed and synthesized eight probes, **5–12**, including 1-amino-2, 6-anhydro-1-deoxy-D-glycero-D-ido-heptitol, which might mimic to a great extent the topography of  $\alpha$ -D-glucopyranoside and modified aglycon of  $\alpha$ -glucopyranoside (Fig. 2).<sup>11</sup> These probes do not have the specific functional groups for glycosidase inhibition, electrostatic interactions (e.g. 1-deoxynojirimycine), transition state mimetic structure (e.g. D-gluconolactone), or covalent bond formation with the enzyme catalytic site (e.g. conduritol B epoxide). The structures of  $\alpha$ -glucosidase inhibitors are summarized in Fig. 3. We investigated the inhibitory activities of family 13 and family 31  $\alpha$ -glucosidases, ER glucosidases, and other glycosidases ( $\beta$ -glucosidase,  $\alpha$ - and  $\beta$ -mannosidase,  $\alpha$ - and  $\beta$ -galactosidase) against probes

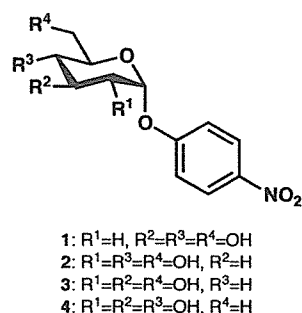


Fig. 1. Chemical structure of glycon profiling probes **1–4**.

**5–12**, and their aglycon specificity profiling was discussed. The values of the % inhibition and IC<sub>50</sub> are summarized in Table 3.<sup>12</sup> Probe **8** indicated specific inhibitions of *Saccharomyces (S.) cerevisiae* (IC<sub>50</sub>=55.5  $\mu$ M) and *Bacillus (B.) stearothermophilus* (IC<sub>50</sub>=415  $\mu$ M)  $\alpha$ -glucosidases. Probe **11** inhibited  $\alpha$ -glucosidase from *S. cerevisiae* (IC<sub>50</sub>=449  $\mu$ M). Honey bee isozyme I (HBG I) was inhibited by probe **5** (IC<sub>50</sub>=851  $\mu$ M). Family 13  $\alpha$ -glucosidases and ER glucosidases were inhibited by the specific probes. On the other hand, family 31  $\alpha$ -glucosidases were broadly inhibited by probes **5–12**. All probes did not inhibit  $\beta$ -glucosidase,  $\alpha$ - or  $\beta$ -mannosidases, or  $\alpha$ - or  $\beta$ -galactosidases at a 5-fold concentration. These facts indicated that aglycon specificities of  $\alpha$ -glucosidases differed greatly among family 13  $\alpha$ -glucosidases, family 31  $\alpha$ -glucosidases and ER glucosidases. Moreover, each aglycon specificity of family 13  $\alpha$ -glucosidases is different in spite of the highly conserved amino acid sequences in the catalytic site.<sup>15</sup> In the kinetic studies on the inhibitions of **8** and **11** and the hydrolysis of PNP  $\alpha$ -Glc by *S. cerevisiae* and *B. stearothermophilus*  $\alpha$ -glucosidases, the values of K<sub>i</sub> and K<sub>m</sub> (mM) were calculated from Dixon plots and Michaelis-Menten plots, respectively, and these values and inhibition types are summarized in Table 4.<sup>12</sup> Probes **8** and **11** were competitive type inhibitors of the *S. cerevisiae* enzyme (K<sub>i</sub>=0.13 mM and 0.50 mM). Probe **8** was a mixed type inhibitor of *B. stearothermophilus* enzyme (K<sub>i</sub>=0.58 mM). The affinities of **8** against both enzymes were higher than PNP  $\alpha$ -Glc as a substrate. These results indicated that probe **8** formed a specific hydrogen bond between the primary hydroxyl group of aglycon moiety and *S. cerevisiae* enzyme, and that probe **11**, with a terminal phenyl group, formed a hydrophobic interaction with the *S. cerevisiae* enzyme.

#### Inhibition of $\alpha$ -glucosidase by reactive oxygen species.

The reactive oxygen species (ROS) generated com-

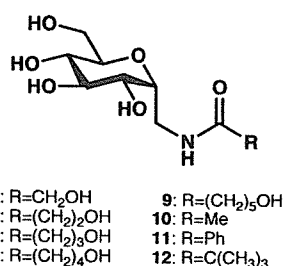
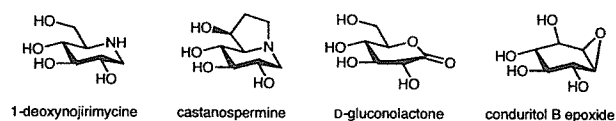
Table 1. Hydrolytic activities and inhibitory activities of probes **1–4** against glucosidases.<sup>11,12)</sup>

Enzyme source	Relative rate of hydrolysis (%) / % Inhibition				
	PNP $\alpha$ -Glc	PNP 2D $\alpha$ -Glc (1)	PNP 3D $\alpha$ -Glc (2)	PNP 4D $\alpha$ -Glc (3)	PNP 6D $\alpha$ -Glc (4)
ER Processing glucosidase					
Rat microsome					
Glucosidase I	- / 56.2	- / 71.7	- / 18.5	- / 22.2	- / 32.3
Glucosidase II	100 / HD	189 / HD	- / -	- / -	- / -
Relative rate of hydrolysis (%)					
$\alpha$ -Glucosidase family 13					
<i>S. cerevisiae</i>	100	-	-	-	-
<i>B. stearothermophilus</i>	100	-	-	-	-
Honey bee I	100	-	-	-	-
Honey bee II	100	-	-	-	-
Honey bee III	100	-	-	-	-
$\alpha$ -Glucosidase family 31					
Rice	100	175	-	-	-
Sugar beet	100	244	-	-	-
Flint corn	100	231	3.7	-	-
<i>A. niger</i>	100	259	11.9	-	-

Relative rate of hydrolysis was expressed by comparison with the amount of *p*-nitrophenol that was released from PNP  $\alpha$ -Glc, which was taken as 100%. Assay of glucosidase I inhibitory activities used [<sup>3</sup>H] glucose-labeled VSV glycoprotein as a substrate. -, Hydrolytic or inhibitory activity was not detected, HD, Hydrolyzing activity was observed.

**Table 2.** Kinetic study of hydrolysis of family 31  $\alpha$ -glucosidases and ER glucosidase II.<sup>9,11)</sup>

Enzyme / Substrate	$K_m$ (mM)	$V_{max}$ ( $\mu\text{mol}/\text{min}/\text{U}$ )	$V_{max}/K_m$
ER glucosidase II			
PNP $\alpha$ -Glc	0.92	1.12	1.23
PNP 2D $\alpha$ -Glc (1)	0.76	3.44	4.53
Enzyme / Substrate	$K_m$ (mM)	$k_{cat}$ ( $\text{s}^{-1}$ )	$k_{cat} / K_m$
Rice $\alpha$ -glucosidase			
PNP $\alpha$ -Glc	2.62	43.8	16.7
PNP 2D $\alpha$ -Glc (1)	6.66	237	35.6
Sugar beet $\alpha$ -glucosidase			
PNP $\alpha$ -Glc	1.04	0.071	0.068
PNP 2D $\alpha$ -Glc (1)	5.70	0.64	0.11
Flint corn $\alpha$ -glucosidase			
PNP $\alpha$ -Glc	0.88	2.00	2.27
PNP 2D $\alpha$ -Glc (1)	7.38	17.0	2.30
PNP 3D $\alpha$ -Glc (2)	9.98	0.44	0.044
<i>A. niger</i> $\alpha$ -glucosidase			
PNP $\alpha$ -Glc	0.59	3.44	5.83
PNP 2D $\alpha$ -Glc (1)	6.09	96.9	15.9
PNP 3D $\alpha$ -Glc (2)	10.2	4.23	0.41

**Fig. 2.** Chemical structure of aglycon profiling probes 5–12.**Fig. 3.** Chemical structure of typical  $\alpha$ -glucosidase inhibitor.**Table 3.** Inhibitory activities of probes 5–12 against glycosidases.<sup>12)</sup>

Enzyme source	% Inhibition ( $IC_{50}$ )							
	5	6	7	8	9	10	11	12
Family 13 $\alpha$ -glucosidase								
<i>S. cerevisiae</i>	<1.0	21.1	<1.0	100 (55.5 $\mu\text{M}$ )	<1.0	<1.0	67.4 (449 $\mu\text{M}$ )	6.1
<i>B. stearothersophilus</i>	<1.0	<1.0	<1.0	100 (415 $\mu\text{M}$ )	<1.0	<1.0	<1.0	<1.0
Honey bee I	52.3 (851 $\mu\text{M}$ )	<1.0	<1.0	37.5	<1.0	10.4	4.6	<1.0
Honey bee II	4.4	2.7	3.6	21.4	4.4	<1.0	12.3	<1.0
Honey bee III	<1.0	3.2	<1.0	<1.0	<1.0	<1.0	<1.0	<1.0
Family 31 $\alpha$ -glucosidase								
Rice	10.7	8.5	7.6	18.3	26.0	21.8	16.0	3.8
Sugar beet	6.9	1.7	3.6	3.1	11.9	8.8	9.8	3.2
Flint corn	29.1	14.1	18.5	37.0	44.6	31.0	49.2	5.6
<i>A. niger</i>	6.6	2.6	<1.0	6.8	<1.0	23.3	14.0	1.2
ER processing glucosidase								
Glucosidase I	<1.0	<1.0	<1.0	<1.0	<1.0	<1.0	18.2	<1.0
Glucosidase II	<1.0	<1.0	<1.0	<1.0	<1.0	<1.0	5.9	<1.0
$\beta$ -Glucosidase	<1.0	<1.0	<1.0	<1.0	<1.0	<1.0	<1.0	<1.0
$\alpha$ -Mannosidase	<1.0	<1.0	<1.0	<1.0	<1.0	<1.0	<1.0	<1.0
$\beta$ -Mannosidase	<1.0	<1.0	<1.0	<1.0	<1.0	<1.0	<1.0	<1.0
$\alpha$ -Galactosidase	<1.0	<1.0	<1.0	<1.0	<1.0	<1.0	<1.0	<1.0
$\beta$ -Galactosidase	<1.0	<1.0	<1.0	<1.0	<1.0	<1.0	<1.0	<1.0

Probe concentrations (family 13 and 31  $\alpha$ -glucosidases: 1  $\mu\text{mol}/\text{mL}$ , ER processing  $\alpha$ -glucosidases: 2  $\mu\text{mol}/\text{mL}$ ,  $\beta$ -glucosidase, mannosidases and galactosidases: 5  $\mu\text{mol}/\text{mL}$ ). Substrate (family 13 and 31  $\alpha$ -glucosidases, ER glucosidase II: PNP  $\alpha$ -Glc, ER glucosidases I: [<sup>3</sup>H] glucose-labeled vesicular stomatitis virus glycoprotein,  $\beta$ -glucosidase: PNP  $\beta$ -Glc,  $\alpha$ -mannosidase: PNP  $\alpha$ -Man,  $\beta$ -mannosidase: PNP  $\beta$ -Man,  $\alpha$ -galactosidase: PNP  $\alpha$ -Gal,  $\beta$ -galactosidase: PNP  $\beta$ -Gal).

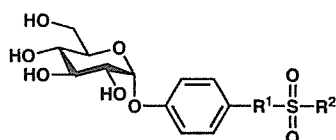
pounds, 13–24, shown in Fig. 4, were assessed as inhibitors of glycoside hydrolase family 13  $\alpha$ -glucosidases and family 31  $\alpha$ -glucosidases,<sup>16)</sup> and the results are listed in Table 5 (Preparation for publication). Compounds 18 and 24, with a terminal  $\alpha$ -naphthyl group, indicated inhibitions of  $\alpha$ -glucosidases from *S. cerevisiae* ( $IC_{50}$ =51.7  $\mu\text{M}$  and  $IC_{50}$ =74.1  $\mu\text{M}$ ) and *B. stearothersophilus* ( $IC_{50}$ =60.1  $\mu\text{M}$  and  $IC_{50}$ =89.1  $\mu\text{M}$ ). We reasoned that the enzymatic liberation of the aglycon from compounds 18 and 24 might be followed by the ejection of a sulfinate anion with the concomitant formation of *p*-benzoquinone and *p*-benzoquinone imine, which would then generate ROS in the enzyme active site, leading to enzyme deactivation.<sup>16,17)</sup> Therefore, the effects of compounds 18 and 24 on ROS-mediated DNA breakage were investigated. DNA strand scission in the super coiled pBR322DNA was induced by ROS in the presence of *p*-benzoquinone or *p*-benzoquinone imine, metal ion, and NADH.<sup>17)</sup> Compound 24 induced DNA strand breakage condition in the above conditions (data not shown). We suggest that ROS-generated enzyme inhibition might be a new approach for the development of an enzyme inhibitor.

#### Inhibition of $\alpha$ -glucosidase by catechin derivatives.

The catechin derivatives 25–33 shown in Fig. 5 were assessed as inhibitors of family 13 and family 31  $\alpha$ -glucosidases, and the results are listed in Table 6.<sup>18)</sup> A comparison of the results against family 13 and family 31  $\alpha$ -glucosidases shows that family 13  $\alpha$ -glucosidases were remarkably inhibited by catechin derivatives compared with family 31  $\alpha$ -glucosidases. The potent inhibition of family 13  $\alpha$ -glucosidases, *S. cerevisiae* and *B. stearothersophilus*, shown by catechin derivative 25 ( $IC_{50}$ =1.2  $\mu\text{M}$  and  $IC_{50}$ =0.7  $\mu\text{M}$ ) and 30 ( $IC_{50}$ =0.9  $\mu\text{M}$  and  $IC_{50}$ =1.1  $\mu\text{M}$ ), are in contrast to the weak activity shown by cate-

**Table 4.** Kinetic studies of the inhibition of family 13  $\alpha$ -glucosidases.<sup>12)</sup>

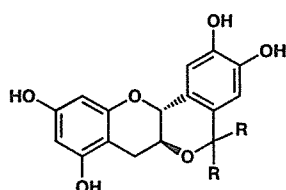
Probe	<i>S. cerevisiae</i>		<i>B. stearothermophilus</i>	
	$K_i$ (mM)	Inhibition type	$K_i$ (mM)	Inhibition type
<b>8</b>	0.13	Competitive	0.58	Mixed
<b>11</b>	0.50	Competitive	—	—
PNP $\alpha$ -Glc	0.35*	—	1.16*	—

\* $K_m$  value.

- 13:** R<sup>1</sup>=O, R<sup>2</sup>=NO<sub>2</sub>      **19:** R<sup>1</sup>=NH, R<sup>2</sup>=NO<sub>2</sub>  
**14:** R<sup>1</sup>=O, R<sup>2</sup>=Cl        **20:** R<sup>1</sup>=NH, R<sup>2</sup>=Cl  
**15:** R<sup>1</sup>=O, R<sup>2</sup>=CF<sub>3</sub>       **21:** R<sup>1</sup>=NH, R<sup>2</sup>=CF<sub>3</sub>  
**16:** R<sup>1</sup>=O, R<sup>2</sup>=CH<sub>3</sub>       **22:** R<sup>1</sup>=NH, R<sup>2</sup>=CH<sub>3</sub>  
**17:** R<sup>1</sup>=O, R<sup>2</sup>=C(CH<sub>3</sub>)<sub>3</sub>   **23:** R<sup>1</sup>=NH, R<sup>2</sup>=C(CH<sub>3</sub>)<sub>3</sub>  
**18:** R<sup>1</sup>=O, R<sup>2</sup>= $\alpha$ -naphthyl   **24:** R<sup>1</sup>=NH, R<sup>2</sup>= $\alpha$ -naphthyl

**Fig. 4.** Chemical structure of ROS-generated compounds 13–24.**Table 5.** Inhibitory activity of ROS-generated compounds 13–24 against  $\alpha$ -glucosidases.

Compound	IC <sub>50</sub> ( $\mu$ M)		
	Glycoside hydrolase family 13		Glycoside hydrolase family 31
	<i>S. cerevisiae</i>	<i>B. stearothermophilus</i>	Rice
<b>13</b>	499	>500	>500
<b>14</b>	437	>500	>500
<b>15</b>	407	>500	>500
<b>16</b>	499	>500	>500
<b>17</b>	391	>500	>500
<b>18</b>	51.7	60.1	>500
<b>19</b>	239	218	>500
<b>20</b>	200	254	>500
<b>21</b>	146	244	>500
<b>22</b>	231	325	>500
<b>23</b>	136	237	>500
<b>24</b>	74.1	89.1	>500



- 25:** R=CH<sub>3</sub>  
**26:** R=CH<sub>2</sub>CH<sub>3</sub>  
**27:** R=(CH<sub>2</sub>)<sub>2</sub>CH<sub>3</sub>  
**28:** R=(CH<sub>2</sub>)<sub>3</sub>CH<sub>3</sub>  
**29:** R=(CH<sub>2</sub>)<sub>4</sub>CH<sub>3</sub>  
**30:** R=(CH<sub>2</sub>)<sub>5</sub>CH<sub>3</sub>  
**31:** R=(CH<sub>2</sub>)<sub>6</sub>CH<sub>3</sub>  
**32:** R=(CH<sub>2</sub>)<sub>7</sub>CH<sub>3</sub>  
**33:** R=(CH<sub>2</sub>)<sub>8</sub>CH<sub>3</sub>

**Fig. 5.** Chemical structure of catechin derivatives 25–33.

chin derivative **26**, which has one methylene group long alkyl side chain compared with **25** (IC<sub>50</sub>=47.5  $\mu$ M and IC<sub>50</sub>=26.8  $\mu$ M) and catechin derivative **33** which has three methylene groups long alkyl side chain compared with **30** (IC<sub>50</sub>=64.0  $\mu$ M and IC<sub>50</sub>=28.1  $\mu$ M). From these results, it is thought that the inhibition mechanism of catechin derivative **25** and the inhibition mechanism of catechin derivative **30** are different. The IC<sub>50</sub> values of typical  $\alpha$ -glucosidase inhibitor 1-deoxynojirimycin (see Fig. 3) and catechin derivative **30** against *S. cerevisiae*  $\alpha$ -glucosidase

**Table 6.** Inhibitory activity of catechin derivatives 25–33 against  $\alpha$ -glucosidases.<sup>18)</sup>

Compound	IC <sub>50</sub> ( $\mu$ M)			
	Glycoside hydrolase family 13		Glycoside hydrolase family 31	
	<i>S. cerevisiae</i>	<i>B. stearothermophilus</i>	Rice	<i>A. niger</i>
Catechin	>500	>500	>500	>500
<b>25</b>	1.2	0.7	>500	>500
<b>26</b>	47.5	26.8	>500	>500
<b>27</b>	37.5	28.4	>500	>500
<b>28</b>	2.1	14.2	>500	>500
<b>29</b>	5.3	6.8	248	>500
<b>30</b>	0.9	1.1	>500	>500
<b>31</b>	4.9	21.1	>500	>500
<b>32</b>	33.2	13.8	>500	>500
<b>33</b>	64.0	28.1	>500	>500

were 3.3<sup>19)</sup> and 0.9  $\mu$ M, respectively. This result indicated that catechin derivative **30** is about 3.6 times more potent than 1-deoxynojirimycin when their IC<sub>50</sub> values are compared.

#### Anti-viral activity of $\alpha$ -glucosidase inhibitors.

Compounds **1–33** were assayed with regard to their ability to inhibit glycoprotein processing at the cellular level. Vesicular stomatitis virus glycoprotein (VSV G) was prepared from VSV-infected and probe-treated baby hamster kidney (BHK) cells.<sup>11)</sup> Analyses of the *N*-glycan structure of obtained VSV G using endo H, which is known to have hydrolytic activity against high-mannose type *N*-glycan, failed to confirm that compounds **1–24** except for catechin derivatives (**25–33**) inhibited processing glycosidases. The catechin derivatives had the possibility of inhibition of processing glycosidases (data not shown). Then, we assayed the anti-virus activities by effects of the catechin derivatives of processing glycosidases on virus glycoprotein synthesis and syncytium formation after new-castle disease virus (NDV) infection, and effects on synthesis and cell surface expression of NDV glycoprotein, hemagglutinin-neuraminidase (HANA) glycoprotein in whole cell lysates were quantified. Moreover, viral infectivity was determined by a plaque assay in BHK cells.<sup>20)</sup> In the above assays, catechin derivative **30** showed potent inhibition of the viral infectivity (Table 7, Preparation for publication).

#### Conclusion and perspectives.

The discovery of glucosidase inhibitors may help us to understand the roles of the oligosaccharides of glycoproteins and glycolipids in cellular functions, and pharmaceutical applications. From this study, it is better to use enzymes of target tissues or organs for the screening of agents for viral diseases, cancer and diabetes. Moreover, in applying glucosidases as inhibitors of glycoprotein processing, inhibitory action of many inhibitors at the cellular levels is not so remarkable, as expected based on their action at the enzyme level. This was speculated to be caused by the difficulty for inhibitors to be able to access the site of action. We think that high throughput

**Table 7.** Anti-viral activity of catechin derivatives at the cellular level.

Compound	Conc. ( $\mu\text{M}$ )	% HAU	SF	% PFU	CPU
Catechin	500	100	+	95	+
	250	100	+	100	+
	125	100	+	NT	+
	63	100	+	NT	+
25	500	0	-	0	+
	250	6	-	14	+
	125	100	+	100	+
	63	100	+	100	+
26	500	0	-	0	-
	250	0	-	0	+
	125	100	+	24	+
	63	100	+	85	+
27	500	0	-	0	-
	250	0	-	0	-
	125	0	-	0	-
	63	100	+	90	+
28	500	0	-	0	-
	250	0	-	0	-
	125	0	-	0	-
	63	100	+	90	+
29	500	0	-	0	-
	250	0	-	0	-
	125	0	-	0	-
	63	100	+	50	-
	31	100	+	100	+
	16	100	+	100	+
30	500	0	-	0	-
	250	0	-	0	-
	125	0	-	0	-
	63	9	+/-	25	-
	31	100	+	95	+
	16	100	+	100	+
33	500	0	-	0	-
	250	0	-	0	-
	125	25	-	50	-
	63	100	+	100	+

screening assays using specific probes and enzymes of target tissues or organs and highly effective design and synthesis of inhibitors *in silico* are necessary for the development of new and potent glucosidase inhibitors.

The authors express sincere thanks to Dr. Seiya Chiba and Dr. Atsuo Kimura for their advice and for some of the  $\alpha$ -glucosidases. We thank Ezaki Glico Co., Ltd. for the gift of  $\alpha$ -arbutin. This work was performed at the Special Postdoctoral Researchers Program (RIKEN). This research was partially supported by a Ministry of Education, Science, Sports and Culture, Grant-in-Aid for Young Scientists (B), 17790097, 2005.

## REFERENCES

- 1) S. Chiba: *Handbook of Amylases and Related Enzymes*, Amylase Research Society of Japan, eds., Pergamon, Oxford, pp. 104-116 (1988).
- 2) T.P. Frandesn and B. Svensson: Plant  $\alpha$ -glucosidases of the glycoside hydrolase family 31. Molecular properties, substrate specificity, reaction mechanism, and comparison with family members of different origin. *Plant Molecul. Biol.*, **37**, 1-13 (1998).
- 3) G.J. Davies and B. Henrissat: Structural enzymology of carbohydrate-active enzymes: implications for the post-genomic era. *Biochem. Soc. Trans.*, **30**, 291-297 (2001).
- 4) Y. Bourne and B. Henrissat: Glycoside hydrolases and glycosyltransferases: families and functional modules. *Curr. Opin. Struct. Biol.*, **11**, 593-600 (2001).
- 5) A. Mehta, N. Zitzmann, P.M. Rudd, T.M. Block, R.A. Dwek:  $\alpha$ -Glucosidase inhibitors as potential broad based anti-viral agents. *FEBS Lett.*, **430**, 17-22 (1998).
- 6) R.A. Dwek, T.D. Butters, F.M. Platt and N. Zitzmann: Targeting glycosylation as a therapeutic approach. *Nat. Rev. Drug Discovery*, **1**, 65-75 (2002).
- 7) W. Hakamata, T. Nishio and T. Oku: Synthesis of *p*-nitrophenyl 3- and 6-deoxy- $\alpha$ -D-glucopyranosides and their specificity to rice  $\alpha$ -glucosidase. *J. Appl. Glycosci.*, **46**, 459-463 (1999).
- 8) W. Hakamata, T. Nishio, R. Sato, T. Mochizuki, K. Tsuchiya, M. Yasuda and T. Oku: Synthesis of monomethyl derivatives of *p*-nitrophenyl  $\alpha$ -D-gluco, galacto, and mannopyranosides and their hydrolytic properties against  $\alpha$ -glucosidase. *J. Carbohydr. Chem.*, **19**, 359-377 (2000).
- 9) T. Nishio, W. Hakamata, A. Kimura, S. Chiba, A. Takatsuki, R. Kawachi and T. Oku: Glycon specificity profiling of  $\alpha$ -glucosidases using monodeoxy and mono-*O*-methyl derivatives of *p*-nitrophenyl  $\alpha$ -D-glucopyranoside. *Carbohydr. Res.*, **337**, 629-634 (2002).
- 10) T. Nishio, W. Hakamata, M. Ogawa, K. Nakajima, Y. Matsuishi, R. Kawachi and T. Oku: Investigations of useful  $\alpha$ -glucosidase for the enzymatic synthesis of rare sugar oligosaccharides. *J. Appl. Glycosci.*, **52**, 153-160 (2005).
- 11) W. Hakamata, M. Muroi, T. Nishio, T. Oku and A. Takatsuki: Recognition properties of processing  $\alpha$ -glucosidase I and  $\alpha$ -glucosidase II. *J. Carbohydr. Chem.*, **23**, 27-39 (2004).
- 12) W. Hakamata, M. Muroi, K. Kadokura, T. Nishio, T. Oku, A. Kimura, S. Chiba and A. Takatsuki: Aglycon specificity profiling of  $\alpha$ -glucosidases using synthetic probes. *Bioorg. Med. Chem. Lett.*, **15**, 1489-1492 (2005).
- 13) W. Hakamata, T. Nishio and T. Oku: Hydrolytic activity of  $\alpha$ -galactosidase against deoxy derivatives of *p*-nitrophenyl  $\alpha$ -D-galactopyranoside. *Carbohydr. Res.*, **324**, 107-115 (2000).
- 14) T. Nishio, Y. Miyake, H. Tsujii, W. Hakamata, K. Kadokura and T. Oku: Hydrolytic activity of  $\alpha$ -mannosidase against deoxy derivatives of *p*-nitrophenyl  $\alpha$ -D-mannopyranoside. *Biosci. Biotechnol. Biochem.*, **60**, 2038-2042 (1996).
- 15) A. Kimura: Molecular anatomy of  $\alpha$ -glucosidase, *Trends Glycosci. Glycotechnol.*, **12**, 373-380 (2000).
- 16) J.C. Briggs, A.H. Haines and R.J.K. Taylor: 4-(Sulfonylamino) phenyl  $\alpha$ -D-glucopyranosides as competitive inhibitors of yeast  $\alpha$ -glucosidase. *J. Chem. Soc., Chem. Commun.*, **18**, 1410-1411 (1993).
- 17) K. Fukuhara, I. Nakanishi, H. Kansui, E. Sugiyama, M. Kimura, T. Shimada, S. Urano, K. Yamaguchi and N. Miyata: Enhanced radical-scavenging activity of a planar catechin analogue. *J. Am. Chem. Soc.*, **124**, 5952-5953 (2002).
- 18) W. Hakamata, I. Nakanishi, Y. Masuda, T. Shimizu, H. Higuchi, Y. Nakamura, T. Oku, S. Saito, S. Urano, T. Ozawa, N. Ikota, N. Miyata, H. Okuda and K. Fukuhara: Planar catechin analogues with alkyl side chain, a potent antioxidant and  $\alpha$ -glucosidase inhibitor. *J. Am. Chem. Soc.* (2006). (in press)
- 19) A.B. Hughes and A.J. Rudge: Deoxynojirimycin: synthesis and biological activity. *Nat. Prod. Rep.*, **11**, 135-162 (1994).
- 20) E. Tsujii, M. Muroi, N. Shiragami and A. Takatsuki: Nectrisine is a potent inhibitor of  $\alpha$ -glucosidases, demonstrating activities similarly at enzyme and cellular levels. *Biochem. Biophys. Res. Commun.*, **220**, 459-466 (1996).

### N-結合型糖鎖プロセッシング酵素を 分子標的とした創薬

袴田 航<sup>1</sup>, 室井 誠<sup>2</sup>, 西尾俊幸<sup>3</sup>, 奥 忠武<sup>3</sup>,  
高月 昭<sup>4</sup>, 長田裕之<sup>3</sup>, 福原 潔<sup>1</sup>, 奥田晴宏<sup>1</sup>,  
栗原正明<sup>1</sup>

<sup>1</sup> 国立医薬品食品衛生研究所有機化学部  
(158-8501 東京都世田谷区上用賀 1-18-1)

<sup>2</sup> 理化学研究所長田抗生物質研究室  
(351-0198 和光市広沢 2-1)

<sup>3</sup> 日本大学生物資源科学部農芸化学科  
(252-8510 藤沢市亀井野 1866)

<sup>4</sup> 法政大学工学部生命機能科学科  
(184-8584 小金井市梶野町 3-7-2)

現在, 新 H5N1 型インフルエンザや SARS など続々と出現する新興ウイルス感染症や鳥インフルエンザのヒトへの伝播等, 新興ウイルス感染症は人類の脅威となっている。しかし, ウイルス感染症に対する有効な薬剤の開発は, 細菌感染症の抗生物質に比べ遅れている。そこで, ウイルス共通の感染機序に基づいた薬剤の開発が重要と考え, 外被を有する多くのウイルスの感染・増殖には複合型の N-結合型糖鎖が関与している知見を基にして, 小胞体 N-結合型糖鎖プロセッシング酵素を標的酵素とした分子標的薬の開発を目指して研究を行っている。分子標的薬の開発には, 標的酵素である糖鎖プロセッシング酵素の基質特異性の解明が必要であると考えた。そこで, 合成プローブを用いて N-結合型糖鎖プロセッシングの第 1 段階を担うプロセッシンググルコシダーゼ I (EC 3.2.1.106) と第 2 段階を担うプロセッシンググルコシダーゼ II (EC 3.2.1.84) のグリコンおよびアグリコン特異性を調べ,  $\alpha$ -グルコシダーゼ (EC 3.2.1.20, GH13 and GH31) のそれと比較した。その結果, グルコシダーゼ I のグリコン特性は GH13  $\alpha$ -グルコシダーゼと, グルコシダーゼ II のグリコン特性は GH31  $\alpha$ -グルコシダーゼと同様であった。またグルコシダーゼ I とグルコシダーゼ II のアグリコン認識は同様であり, GH13 および GH31  $\alpha$ -グルコシダーゼとは異なっていた。そこで, プロセッシンググルコシダーゼ I および II を標的として, 酵素阻害剤候補化合物の設計と合成を行った。これら候補化合物の *in vitro* 酵素阻害活性と細胞レベルでのウイルス外被糖タンパク質の合成・成熟・転送阻害およびプラーク法による感染性ウイルス数の測定を行った。その結果, *in vitro* においてヘプチトール誘導体, スルフォニル誘導体の一部に IC<sub>50</sub> 約 50  $\mu$ M の阻害活性を, カテキン誘導体の一部に IC<sub>50</sub> 0.9  $\mu$ M の強力な阻害活性を見いだした。さらに, 細胞レベルではカテキン誘

導体の一部にプロセッシンググルコシダーゼ阻害を作用点とするとみられる比較的強い抗ウイルス活性を見いだした。今後, ウイルス外被糖タンパク質の糖鎖構造解析等により詳細な作用機序の解明を行う予定である。

\*\*\*\*\*

〔質問〕

食総研 徳安

- 1) 安全性の高いカテキン骨格をリード化合物として, カテキン骨格を含む阻害剤の設計と合成を行っています。その阻害剤の「安全性が高い」という理由はなにか。
- 2) ウイルスに対してカテキン誘導体の効果があったが,  $\alpha$ -グルコシダーゼに対して作用した結果なのか。

〔答〕

1) 誘導体合成前のカテキンの安全性が高いからといって, カテキン骨格を有する誘導体の安全性が高いということではできません。しかし, 安全性の高い骨格を創薬リード化合物として用いることは, 毒性を回避するという目的において理にかなっていると考えています。また, 本誘導体はカテキン骨格をほぼ維持しているため, 毒性発現の可能性を低く抑えられるのではないかと考えております。

2)  $\alpha$ -グルコシダーゼに対する阻害効果なのかどうか, 直接の証拠はありませんが, *in vitro* での強い阻害活性およびウイルスを感染させた培養細胞の形態から  $\alpha$ -グルコシダーゼ阻害を作用機序とする抗ウイルス作用であると考えております。今後, ウイルス粒子を回収し, そのウイルス外被糖タンパク質の糖鎖解析を行うことにより, 作用点を解明したいと考えております。

〔質問〕

食総研 北岡

- 1) グルコシダーゼ阻害剤のリード化合物として, 数ある安全性の高い物質の中から, カテキンを選択した理由はなにか。
- 2) グルコシダーゼ以外の糖質加水分解酵素の阻害剤になっている可能性はあるのでしょうか。

〔答〕

1) 安全性の高い物質は他にもたくさんありますが, カテキンには弱いながらも血糖上昇抑制作用が報告されており, 腸管グルコシダーゼ阻害が示唆されておりますので, リード化合物として選択いたしました。

2) グルコシダーゼ阻害以外の阻害活性があることは否定できません。現時点では, 一部の  $\alpha$ -マンノシダーゼに対する阻害活性がないことだけ確認しております。



## Structural basis for DNA-cleaving activity of resveratrol in the presence of Cu(II)

Kiyoshi Fukuhara,<sup>a,\*</sup> Maki Nagakawa,<sup>b</sup> Ikuo Nakanishi,<sup>c,d</sup> Kei Ohkubo,<sup>d</sup> Kohei Imai,<sup>e</sup> Shiro Urano,<sup>e</sup> Shunichi Fukuzumi,<sup>d</sup> Toshihiko Ozawa,<sup>c</sup> Nobuo Ikota,<sup>c</sup> Masataka Mochizuki,<sup>b</sup> Naoki Miyata<sup>f</sup> and Haruhiro Okuda<sup>a</sup>

<sup>a</sup>Division of Organic Chemistry, National Institute of Health Sciences, 1-18-1 Setagaya-ku, Tokyo 158-8501, Japan

<sup>b</sup>Division of Organic and Bioorganic Chemistry, Kyoritsu University of Pharmacy, 1-5-30 Shibakoen, Minato-ku, Tokyo 105-8512, Japan

<sup>c</sup>Redox Regulation Research Group, Research Center for Radiation Safety, National Institute of Radiological Sciences (NIRS), 4-9-1 Anagawa, Inage-ku, Chiba 263-8555, Japan

<sup>d</sup>Department of Material and Life Science, Graduate School of Engineering, Osaka University, SORST, Japan Science and Technology Agency (JST), 2-1 Yamada-oka, Suita, Osaka 565-0871, Japan

<sup>e</sup>Department of Applied Chemistry, Shibaura Institute of Technology, Minato-ku, Tokyo 108-8548, Japan

<sup>f</sup>Graduate School of Pharmaceutical Sciences, Nagoya City University, 3-1 Tanabe-dori, Mizuho-ku, Nagoya, Aichi 467-8603, Japan

Received 31 August 2005; revised 27 September 2005; accepted 27 September 2005

Available online 24 October 2005

**Abstract**—Resveratrol (**1**, 3,5,4'-trihydroxy-*trans*-stilbene), a polyphenol found in grapes and other food products, is known as an antioxidant and cancer chemopreventive agent. However, **1** was shown to induce genotoxicity through a high frequency of micronucleus and sister chromatid exchange in vitro and DNA-cleaving activity in the presence of Cu(II). The present study was designed to explore the structure–activity relationship of **1** in DNA strand scission and to characterize the substrate specificity for Cu(II) and DNA binding. When pBR322DNA was incubated with **1** or its analogues differing in the number and positions of hydroxyl groups in the presence of Cu(II), the ability of 4-hydroxystilbene analogues to induce DNA strand scission is much stronger than that of 3-hydroxy analogues. The high binding affinity with both Cu(II) and DNA was also observed by 4-hydroxystilbene analogues. The reduction of Cu(II) which is essential for activation of molecular oxygen proceeded by addition of **1** to the solution of the Cu(II)–DNA complex, while such reduction was not observed with the addition of isoresveratrol, in which the 4-hydroxy group of **1** is changed to the 3-position. The results show that the 4-hydroxystilbene structure of **1** is a major determinant of generation of reactive oxygen species that was responsible for DNA strand scission.

© 2005 Elsevier Ltd. All rights reserved.

### 1. Introduction

Natural polyphenols, including catechin, epicatechin, quercetin, and resveratrol, are natural antioxidants that are found in a wide range of plant species. Polyphenols inhibit the oxidation of human low-density lipoprotein (LDL),<sup>1</sup> which is responsible for promoting atherogenesis,<sup>2,3</sup> and the intake of foods and beverages that contain polyphenols may protect against atherosclerosis.<sup>4</sup> The polyphenol resveratrol (3,5,4'-trihydroxy-*trans*-stilbene; **1**)

is found in grapes, where it serves as a phytoalexin that protects against fungal infection.<sup>5</sup> Although its biosynthesis is not well defined, **1** is thought to be synthesized in response to infection or injury.<sup>6</sup> Resveratrol **1** (Fig. 1) has some therapeutic effects that are due to its antioxidant potential and originate from the inhibition of the oxidation of human LDL and the reduced propensity of human plasma and LDL to undergo lipid peroxidation.<sup>7,8</sup> In addition to its antioxidant potential, it has also been reported to have a variety of anti-inflammatory, anti-platelet, and anti-carcinogenic effects.<sup>9,10</sup> Therefore, due to its high concentration in grape skin, the beneficial effects of the consumption of red wine at reducing the risk of cardiovascular disease have been attributed to the multiple effects of **1**.<sup>11</sup> Recently, **1** was shown to inhibit cellular events associated with

**Keywords:** Resveratrol; Polyphenol; Antioxidant; DNA oxidative damage.

\* Corresponding author. Tel.: +81-3-3700-1141; fax: +81-3-3707-6950; e-mail: [fukuhara@nihs.go.jp](mailto:fukuhara@nihs.go.jp)

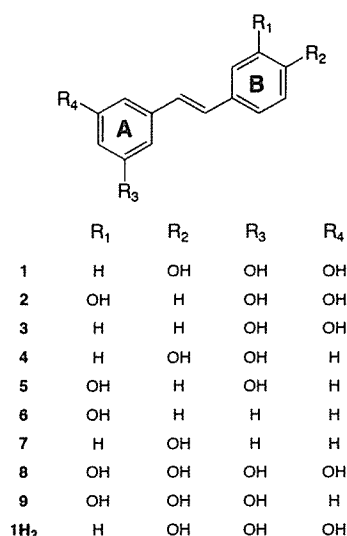


Figure 1. Structure of resveratrol (**1**), its analogues **2–9**, and dihydroresveratrol (**1H<sub>2</sub>**).

tumor initiation, promotion, and progression.<sup>12</sup> Furthermore, it has been reported that **1** has the potential to inhibit DNA polymerase and cyclooxygenase,<sup>13</sup> and also has a direct antiproliferative effect on human breast epithelial cells.<sup>14</sup> Based on its antimutagenic activity,<sup>15,16</sup> it has been suggested that **1** should be effective as a cancer chemopreventive agent in humans.

Meanwhile, 5-alkyl-1,3-dihydroxybenzenes (5-alkylresorcinol) have long been recognized to have potential as therapeutic agents, since natural resorcinols have a wide variety of biological activities, including fungicidal and bactericidal activities against numerous pathogens.<sup>17</sup> Hecht and co-workers were the first to demonstrate that 5-alkylresorcinol induced Cu(II)-dependent DNA strand scission under alkaline pH.<sup>18</sup> This DNA cleavage requires the initial oxygenation of the benzene nucleus, a process that occurs readily at an alkaline pH in the presence of Cu(II) and O<sub>2</sub>. The resulting trihydroxylated benzene mediates DNA cleavage in a reaction that depends on the presence of Cu(II) and O<sub>2</sub>. Recently, based on the similar structures of 5-alkylresorcinol and resveratrol, we suggested that **1** may be able to mediate Cu(II)-dependent DNA strand scission under neutral conditions.<sup>19</sup> Interestingly, DNA strand scission occurred at neutral pH, indicating that **1** can induce

DNA cleavage without the oxygenation of benzene nuclei to the catechol moiety, which is a requisite intermediate in resorcinol-induced DNA cleavage. It has also been shown that DNA cleavage is more likely caused by a copper–peroxide complex as the reactive species rather than by a freely diffusible oxygen species that mediates DNA degradation by resorcinol in the presence of Cu(II). However, instead of the catechol structure, the structural feature of **1** that is effective for DNA cleavage is still unknown. To address this question, the present study was designed to explore the structure–activity relationship of synthesized hydroxystilbene derivatives (Fig. 1) in DNA strand 4 scission and also to characterize the substrate specificity for Cu(II) and DNA binding. The results show that the 4-hydroxy group of **1** is a major determinant of DNA cleaving ability and confirm that the stilbene structure is also important for this ability.

## 2. Result and discussion

### 2.1. DNA-cleaving activity

The ability of **1** and its analogues to induce DNA-cleaving activity was examined using pBR322, a supercoiled, covalently closed circular DNA (Form I), and analyzed by agarose gel electrophoresis. Consistent with the fact that Cu(II) is required for potent DNA-cleaving activity of **1**, the individual hydroxylated stilbenes induced DNA cleavage only when the reaction was carried out in the presence of Cu(II); in the absence of Cu(II), no DNA cleavage was observed (data not shown). Figure 2 shows the results of the analysis in the presence of Cu(II). Replacement of the internal double bond in the stilbene moiety by a saturated one (**1H<sub>2</sub>**) resulted in a marked reduction in potency, suggesting that the structure of stilbene is important for mediating DNA relaxation. In a series of hydroxylated stilbene analogues, Cu(II)-dependent DNA-cleaving activity was greatly affected by the number and positions of hydroxyl groups attached to the stilbene structure. For a given structural series (i.e., all 4-OH analogues: **1**, **4**, **7**; 3-OH analogues: **2**, **3**, **5**, **6**; or 3,4-(OH) analogues: **8**, **9**), the DNA-cleaving activity seemed to increase with an increase in the number of hydroxyl groups. Densitometric analysis of agarose gel indicated that the DNA-cleaving ability of **1** resulted not only in the complete conversion of substrate DNA (Form I) into open circular DNA (Form II) but also the further conversion of Form II into linear

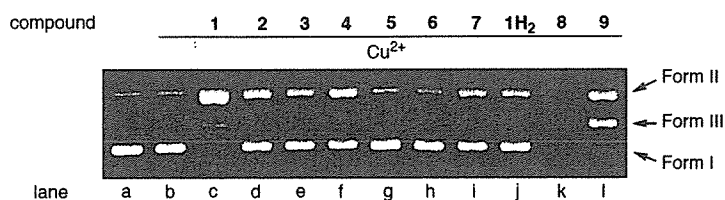


Figure 2. Gel electrophoretic analysis of single- and double-strand breaks generated in pBR322DNA with **1** or its analogues in the presence of Cu(II). Assays were performed in 50 mM sodium cacodylate buffer, pH 7.2, containing 45 μbp pBR322DNA and 10 μM of samples (lane c–l) in the presence of 10 μM Cu(II) (lane b–l), for 1 h at 37 °C. The samples in lane c–l are **1–9**, and **1H<sub>2</sub>**, respectively.

DNA (Form III) in 8% yield. Compounds **8** and **9** were much more efficient at mediating DNA relaxation than **1**; especially, **8** induced the complete degradation of linear DNA (Form III) as indicated by the smearing of the band. The high potency of **8** and **9** can be attributed to their *ortho*-hydroquinone (catechol) structure, which logically improves their ability to cleave DNA by facilitating the generation of oxygen radicals through the formation of *ortho*-hydroquinone–Cu(II)–O<sub>2</sub> complex. Of particular interest is the difference in the potency between **1** and its 3-hydroxy isomer **2**. A change in the placement of the 4-hydroxy group of **1** to the 3-position resulted in a significant decrease in its ability to cleave DNA. Similar differences were noted in comparing the dihydroxy (**4** vs **5**) and monohydroxy (**6** vs **7**) stilbenes, which is consistent with the suggestion that the 4-hydroxy group is essential for effecting DNA cleavage. Since oxygen radical is believed to be the active species responsible for Cu(II)-dependent DNA cleavage, the 4-hydroxy group in combination of O<sub>2</sub> and Cu(II) may serve to facilitate the generation of oxygen radical. However, **3** was found to be quite efficient at mediating DNA relaxation, which suggests that the 3,5-dihydroxybenzene structure, which is distinct from 3-hydroxybenzene, is also essential for potentiating DNA strand scission.

## 2.2. Cu(II)-binding ability

It has been shown that several xenobiotics that contain a catechol moiety undergo Cu(II)-mediated oxidation to form reactive oxygen species (ROS) that are capable of causing DNA strand breaks. Sotomatsu et al. demonstrated that Cu(II) and Fe(III) had affinity for the hydroquinone moiety of 3,4-dihydroxyphenylalanine (dopa) and, after coordinating with dopa, promoted the peroxidative cleavage of unsaturated phospholipids.<sup>20</sup> Since **1** can coordinate Cu(II), its binding ability has been observed as a change in UV absorption spectra using a Cu(II) titration experiment, whereas no such binding has been observed in the case of Fe(III).<sup>8</sup> Considering the unique specificity of Cu(II), which may induce DNA strand scission of **1**, the ability of **1** to bind to Cu(II) might be advantageous for generating ROS and inducing Cu(II)-dependent DNA scission. Therefore, to elucidate the structural component of **1** that is responsible for its Cu(II)-binding ability, the UV spectra of **1** and its analogues (**2–7** and **1H<sub>2</sub>**) in various concentrations of Cu(II) were observed, and their Cu(II)-binding abilities were compared. As shown in Figure 3, the incremental addition of Cu(II) to 20  $\mu$ M of **1** resulted in a blueshift of the peak from 220 to 210 nm with a concomitant increase in absorbance and a decrease in the absorbance at 308 nm, consistent with the binding of **1** with Cu(II). This spectral change reflects a 1:1 stoichiometry for the complex between **1** and Cu(II), and the binding constant was determined to be  $1.75 \times 10^7 \text{ M}^{-1}$ . Figure 4 shows the effect of the Cu(II) concentration on the absorbance of **1** and its analogues in the range 270–330 nm. A decrease in absorbance, similar to that of **1** at 308 nm, was observed for 3,4- and 4-hydroxy analogues of **4** and **7** at 324 and 304 nm, respectively, indicating that the change is due to its coordination with

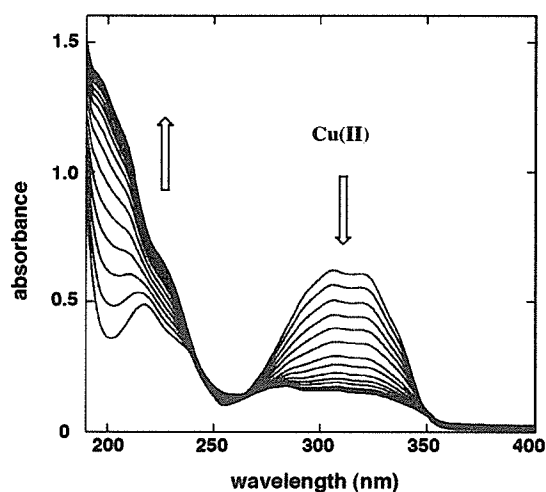


Figure 3. Spectral changes observed upon addition of CuCl<sub>2</sub> (0–30  $\mu$ M) to a sodium cacodylate buffer (pH 7.1)/CH<sub>3</sub>CN mixed solution of **1** (20  $\mu$ M).

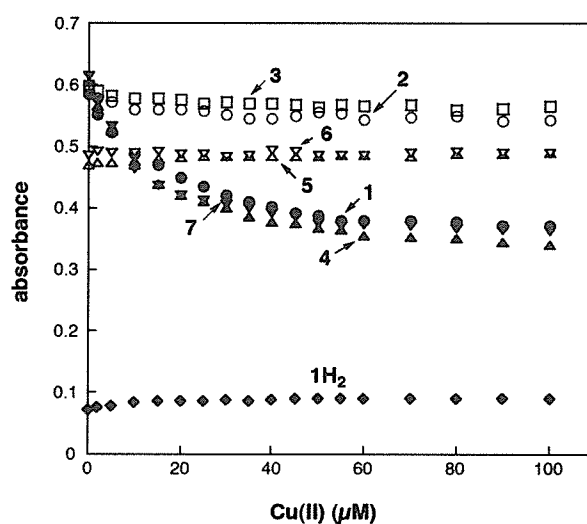
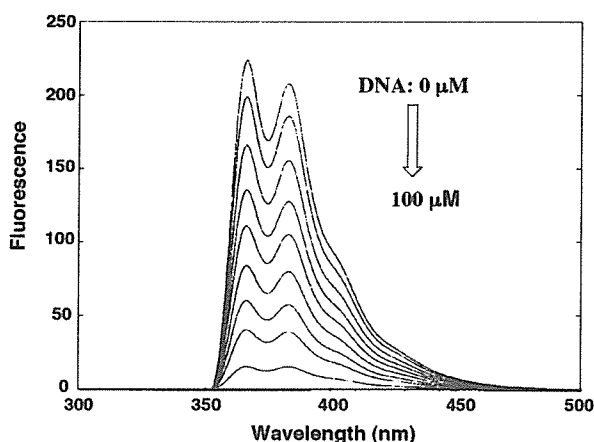


Figure 4. Changes in the absorbance ( $\lambda_{\text{max}}$ ) of **1** and its analogues (20  $\mu$ M) upon the addition of CuCl<sub>2</sub> (0–100  $\mu$ M).

Cu(II). In contrast, with an increase in the concentration of Cu(II), there was little or no effect on the absorbance of **2**, **3**, **5**, and **6**, which lacked a 4-hydroxy group on the stilbene moiety, at 306, 300, 298, and 298 nm, respectively, suggesting that ligation of these compounds to Cu(II) did not occur. Further, only a slight effect was observed for dihydroresveratrol **1H<sub>2</sub>**. These results constitute strong evidence that the 4-hydroxy group of **1** is essential for Cu(II) coordination and the ability of the 4-hydroxy group to bind with Cu(II) depends on the structure of stilbene.

## 2.3. DNA-binding ability

Since **1** is capable of binding to DNA,<sup>19</sup> ROS produced by **1** in combination with Cu(II) might be effective at mediating DNA relaxation. Therefore, to



**Figure 5.** Effect of calf thymus DNA on the fluorescence emission (excitation wavelength 260 nm) of **1**. Trace 1 is the emission spectrum of **1** alone (20  $\mu\text{M}$ ); traces 2–9 are emission spectra of **1** in the presence of 2, 5, 10, 15, 20, 30, 50, and 100  $\mu\text{M}$  DNA bp, respectively.

characterize the interaction of **1** with DNA, the ability of **1** and its analogues to bind DNA was estimated by fluorescence titration. The fluorescence emission spectra of **1** in the presence of calf thymus DNA are shown in Figure 5. As indicated, the addition of DNA to **1** causes a decrease in fluorescence emission, and, without any modification of the spectral shape, a decrease in the degree of fluorescence is seen with an increasing concentration of DNA, suggesting that **1** binds to duplex DNA not via groove binding but rather through significant intercalation. In fact, denatured DNA does not appreciably quench the fluorescence of **1** (data not shown). Stern–Volmer plots of the quenching of the fluorescence of **1** and its analogues (**2–7** and **1H<sub>2</sub>**) by calf thymus DNA are shown in Figure 6. Native DNA quenches the fluorescence of **1** five times more efficiently than it quenches **1H<sub>2</sub>**,

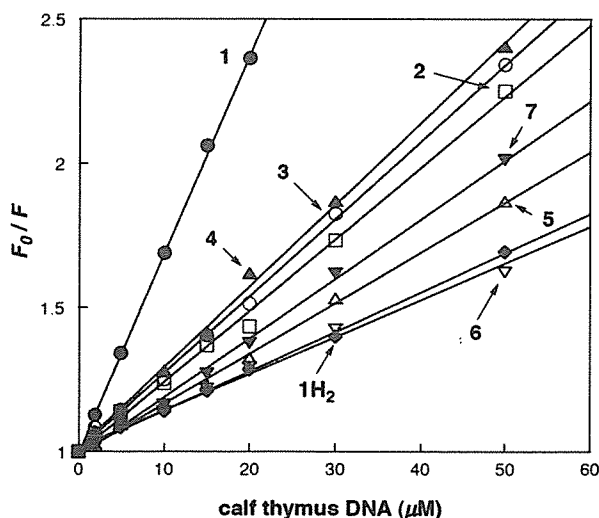


**Figure 6.** Stern–Volmer plot of quenching of the fluorescence of **1** and its analogues by calf thymus DNA.

indicating that the planarity of the stilbene structure is effective for binding with the duplex DNA structure, probably by taking advantage of its stacking against the base pair. Figure 6 also indicates that phenolic hydroxyl groups attached to the stilbene structure greatly affect the DNA-binding affinity. An increase in the number of hydroxyl groups tends to increase the DNA-binding affinity, which is consistent with the suggestion that the number of phenolic hydroxyl groups is important for its DNA-binding affinity. However, the binding affinity is also determined by the combination of the number and localization of phenolic hydroxyl groups. Thus, the fluorescence of isoresveratrol **2**, in which the 4-hydroxy group of resveratrol **1** is changed to the 3-position, was quenched by DNA with low efficiency ( $K_{sv} = 2.40 \times 10^4 \text{ M}^{-1}$ ) compared to **1** ( $K_{sv} = 6.80 \times 10^4 \text{ M}^{-1}$ ), and the same results were also observed with dihydroxyl (**4** vs **5**) and monohydroxyl (**7** vs **6**) stilbenes, suggesting that the 4-hydroxy group may be the essential component for binding DNA and plays an important role in specific hydrogen bond interactions with DNA.

#### 2.4. ESR analysis

To confirm the electrostatic interaction of hydroxylated stilbenes with both Cu(II) and DNA, ESR signals of Cu(II) were observed in the presence of **1** or its analogues together with calf thymus DNA. Once the ternary complex of Cu(II)–**1**–DNA, which is due to the efficient binding affinities of **1** with both Cu(II) and DNA, is formed, the complex may result due to its high DNA-cleaving ability. Figure 7 shows that an ESR signal of Cu(II) became multiple upon the addition of DNA, consistent with the fact that Cu(II) complexes DNA. In fact, the decrease in the peak height of Cu(II) in a solution of calf thymus DNA is due to the intercalation of Cu(II) with a large molecule of DNA, which limits the mobility of Cu(II). When **1** was added to the solution of Cu(II)–DNA complex, the peak height of the ESR signal was reduced to one-half of that of the Cu(II)–DNA complex and the resonance was weakened, suggesting that **1** was bound to Cu(II)–DNA complex and thus induced the reduction of Cu(II), which was converted to an ESR-silent species, very likely Cu(I). If the binding of Cu(II) to DNA decreases with the addition of **1**, the signal of Cu(II) should increase to the height of unbound Cu(II). An increase in peak height was also not observed for other resveratrol analogues, suggesting that Cu(II) remains in a complex with DNA even after the addition of **1** and its analogues. Compared to the reduction of Cu(II) to Cu(I) by **1**, an efficient reduction of the peak height of Cu(II)–DNA complex was not observed with the addition of isoresveratrol **2**. It is possible that the insufficient binding affinity of **2** with both DNA and Cu(II) may impair the highly efficient reduction of Cu(II) to Cu(I). Similarly, **7** affected the spectra of Cu(II)–DNA with efficient reducing and broadening, whereas there was no effect on the spectra of Cu(II)–DNA upon the addition of **6**, indicating that the reductive activation of Cu(II) is accelerated by electrostatic interaction of a hydroxyl group at the 4-position.

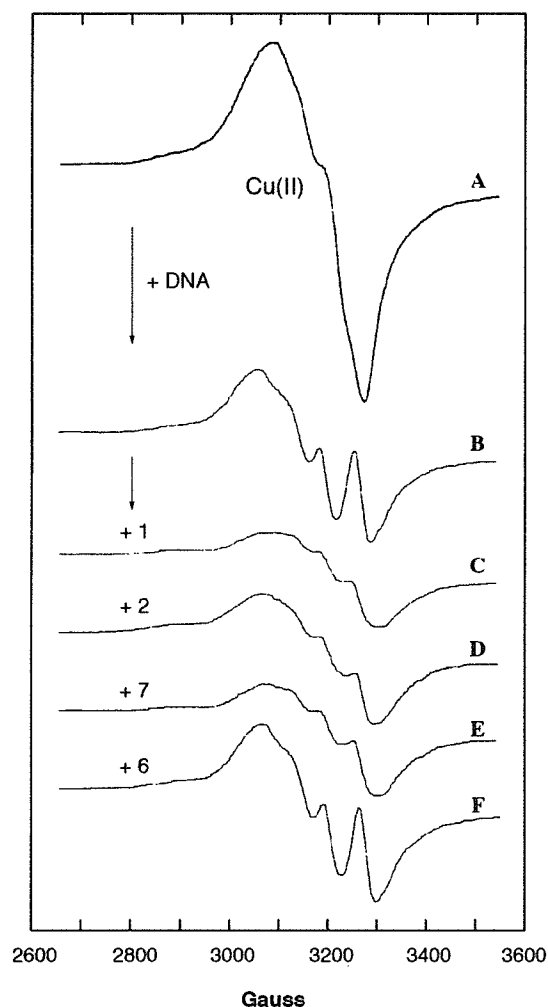


**Figure 7.** Effect of **1** and its analogues on the ESR spectra of Cu(II) in the presence of calf thymus DNA. Spectra A is 1 mM CuCl<sub>2</sub> and spectra B–F show after the addition of 2 mM NP of calf thymus DNA in the absence (B) or presence of 1 mM chemicals (C: **1**; D: **2**; E: **7**; F: **6**). All spectra were recorded after incubation for 30 min at room temperature.

### 3. Conclusion

In general, polyphenols, which are responsible for reactive oxygen-associated toxicity, appear to play an important role in the reductive activation of molecular oxygen by its autooxidation, which, in most cases, is coupled with the formation of redox active *ortho*- or *para*-quinones. Catechol is the typical polyphenol that is essential for generating oxygen radical in the presence of Cu(II).<sup>21</sup> It is formed as an activated metabolite of polycyclic aromatic hydrocarbons, which are known to be ubiquitous environmental pollutants. Although **1** is a polyphenol that is known to be an antioxidant and a potential cancer chemopreventive agent, it cleaved DNA strongly without oxidative transformation to the catechol structure in the presence of Cu(II). The DNA cleavage is attributed to the generation of copper-peroxide complex that is formed by electron transfer from **1** to molecular oxygen.<sup>19</sup> The oxidative product of **1** is a

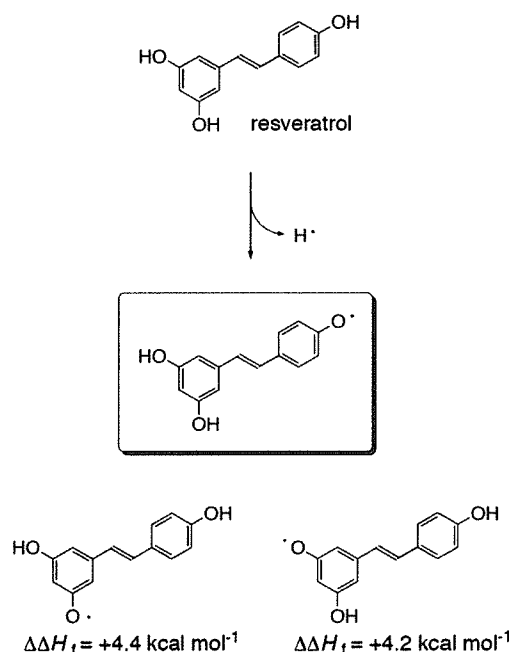


**Figure 8.** Relative energy values ( $\Delta\Delta H_f$ ) of three types of resveratrol radicals calculated by the DFT calculation, B3LYP/6-31G\* basis set.

dimer<sup>22</sup> and formation of the catechol structure has not been reported. Therefore, the oxidative dimer might be formed by dimerization of resveratrol radical as a result of the reductive activation of molecular oxygen. In the present work, the number and positions of the hydroxyl groups in the stilbene structure were associated with DNA-cleaving activity and the 4-hydroxy group of stilbene played an especially critical role in DNA cleavage. The high binding affinity of a hydroxyl group at the 4-position with both Cu(II) and DNA makes it possible to form a ternary complex and therefore cleave DNA efficiently. When the heats of formation of three types of resveratrol radicals are compared, as shown in Figure 8, the 4-oxy radical of **1** is the most stable, indicating that the hydroxyl group at the 4-position is much more subjected to oxidation than other hydroxyl groups. In fact, the efficient reduction of Cu(II) to Cu(I) was seen with **1**, which has a hydroxyl group at the 4-position, while there was no effect on Cu(II) reduction in the presence of **2** in which the 4-hydroxy group in **1** is moved to the 3-position. The decrease in the DNA-cleaving ability of **1H<sub>2</sub>** compared to that of **1** also indicated the importance of the stilbene structure, which might be effective not only for DNA binding for the planarity of the overall structure but also for the stability of the 4-oxy radical. These results suggest that the ability of **1** to induce oxidative DNA damage in the presence of Cu(II) can be attributed to the structure of 4-hydroxystilbene which is comparable to that of catechol.

Estrogens have been reported to cause cancer through a genotoxic effect. The genotoxicity of estrogens is attributed to the accumulation of potentially carcinogenic metabolites and almost all of these are the catechol form of estrogens. Catechol estrogen metabolites are capable

of causing chromosomal aberrations and gene mutations in cultured cells. The oxidative DNA damage and/or alkylation of DNA that is responsible for the risk of developing cancer are also induced by catechol estrogen metabolites. In fact, the catechol structure, which can cause genotoxicity, is capable of inducing DNA strand scission and the oxidation of DNA bases in the presence of Cu(II). Recently, we reported the genotoxicity of **1**, which induced micronucleus, sister chromatid exchange, and S phase arrest.<sup>23</sup> Among the many types of hydroxylated stilbenes, 4-hydroxystilbene most effectively caused genotoxic effects. Therefore, the finding that the 4-hydroxystilbene structure is responsible for various biological activities, especially DNA damage leading to genotoxicity, might be important for understanding the toxicity of polyphenols that do not have a catechol structure.

## 4. Experimental

### 4.1. Materials

Resveratrol **1** and calf thymus DNA were purchased from Sigma (St. Louis, MO). Supercoiled plasmid pBR322DNA was purchased from Nippon Gene (Tokyo, Japan). Analogues of **1**: 3,5,3'-trihydroxy- (**2**), 3,5-dihydroxy- (**3**), 3,4'-dihydroxy- (**4**), 3,3'-dihydroxy- (**5**), 3-hydroxy- (**6**), 4-hydroxy (**7**), 3,4,3',5'-tetrahydroxy- (**8**), and 3,4,3'-trihydroxy-*trans*-stilbene (**9**), as shown in Figure 1, were synthesized as previously reported.<sup>24</sup> Saturated form of **1** (**1H<sub>2</sub>**) was synthesized by hydrogenation of **1** using 10% Pd/C as catalyst. Yield: 98%. <sup>1</sup>H NMR(acetone-*d*<sub>6</sub>):  $\delta$  2.73 (m, 4H), 6.19 (d, 1H,  $J = 2.0$  Hz), 6.22 (d, 1H,  $J = 2.0$  Hz), 6.74 (d, 2H,  $J = 8.4$  Hz), 7.03 (d, 2H,  $J = 8.4$  Hz). All other chemicals and solvents were of reagent grade or better.

### 4.2. DNA-cleaving activity

DNA strand breakage was measured in terms of the conversion of supercoiled pBR322 plasmid DNA to the open circular and linear forms. Reactions were carried out in 20  $\mu$ L (total volume) of 50 mM Na cacodylate buffer (2.5% DMF), pH 7.2, containing 45  $\mu$ M bp pBR322 DNA, 10  $\mu$ M CuCl<sub>2</sub>, and 100  $\mu$ M of each stilbene derivative. The reaction mixtures were incubated at 37 °C for 1 h and then treated with 5  $\mu$ L of loading buffer (100 mM TBE buffer, pH 8.3, containing 30% glycerol, 0.1% bromophenol blue) and applied to 1% agarose gel. Horizontal gel electrophoresis was carried out in 50 mM TBE buffer, pH 8.3. The gels were stained with ethidium bromide (1  $\mu$ g mL<sup>-1</sup>) for 30 min, destained in water for 30 min, and photographed with UV transillumination.

### 4.3. UV-visible spectra measurements

UV-visible spectra were measured at 37 °C with a Hewlett Packard 8452A Diode Array Spectrophotometer. A solution in a final volume of 1 mL consisted of 20  $\mu$ M of sample and 0–100  $\mu$ M CuCl<sub>2</sub> in sodium cac-

odylate buffer (pH 7.1)/acetonitrile mixed solvent (1:1 v/v) was prepared and subjected to spectral analysis. The binding constant between **1** and Cu(II) was obtained according to the method described by Itoh et al.<sup>25</sup>

### 4.4. Fluorescence measurements

Fluorescence excitation and emission spectra were recorded on a Shimadzu RF-5300PC. A solution in a final volume of 1 mL, which consisted of 20  $\mu$ M of sample and 0–100  $\mu$ M calf thymus DNA in 10 mM sodium cacodylate buffer (pH 7.1) and DMF (10% by volume), was used for fluorescence-quenching experiments. The excitation wavelengths used were 255 nm for **1**, **3**, **6**, and **7**, and 260 nm for **2**, **4**, **5**, and **1H<sub>2</sub>**, and emissions were recorded in the range of 300–500 nm. For all experiments, the sample temperature was maintained at 37 °C. The quenching data were analyzed by the Stern–Volmer equation:<sup>26</sup>

$$F_0/F = 1 + K_{sv}[Q],$$

where [Q] is the molar concentration of the calf thymus DNA,  $F_0$  and  $F$  are the fluorescence intensities in the absence and in the presence of the calf thymus DNA [Q], respectively, and  $K_{sv}$  is the Stern–Volmer quenching constant.

### 4.5. ESR analysis

ESR spectra were recorded at room temperature on a JES-FE 2XG spectrometer (JEOL Co. Ltd., Tokyo, Japan). The sample containing 1 mM CuCl<sub>2</sub>, 2 mM NP of calf thymus DNA, and 1 mM of chemical in 50 mM phosphate buffer (pH 7.2) and acetonitrile (5% by volume) was introduced into a quartz flat cell and incubated at room temperature for 30 min. The ESR spectrum was then recorded. The spectrometer settings were modulation frequency, 100 kHz; modulation amplitude, 10 G; and microwave power, 16 mW.

### 4.6. Theoretical calculations

Density functional calculations were performed with Gaussian03 (Revision C.02, Gaussian, Inc.) using the unrestricted B3LYP functional for the open shell molecule on an 8-processor QuantumCube<sup>TM</sup> developed by Parallel Quantum Solutions.

## Acknowledgments

This work was supported partly by a grant (MF-16) from the Organization for Pharmaceutical Safety and Research of Japan, a grant from the Ministry of Health, Labour and Welfare, a Grant-in-Aid for Research of Health Sciences focusing on Drug Innovation (KH51058) from the Japan Health Sciences Foundation, and partly by Grants-in-Aid for Scientific Research (B) (No. 17390033) and for Young Scientist (B) (No. 17790044) from the Ministry of Education, Culture, Sports, Science and Technology, Japan.

## References and notes

1. Hirano, R.; Sasamoto, W.; Matsumoto, A.; Itakura, H.; Igarashi, O.; Kondo, K. *J. Nutr. Sci. Vitaminol. (Tokyo)* **2001**, *47*, 357.
2. Witztum, J. L.; Steinberg, D. *J. Clin. Invest.* **1991**, *88*, 1785.
3. Steinberg, D. *J. Biol. Chem.* **1997**, *272*, 20963.
4. Hayek, T.; Fuhrman, B.; Vaya, J.; Rosenblat, M.; Belinky, P.; Coleman, R.; Elis, A.; Aviram, M. *Arterioscler. Thromb. Vasc. Biol.* **1997**, *17*, 2744.
5. Jeandet, P.; Bessis, R.; Gautheron, B. *Am. J. Enol. Vitic.* **1991**, *42*, 41.
6. Langcake, P.; Pryce, R. *J. Physiol. Plant Pathol.* **1976**, *9*, 77.
7. Frankel, E. N.; Waterhouse, A. L.; Kinsella, J. E. *Lancet* **1993**, *341*, 1103.
8. Belguendouz, L.; Fremont, L.; Linard, A. *Biochem. Pharmacol.* **1997**, *53*, 1347.
9. Jang, M.; Pezzuto, J. M. *Drugs Exp. Clin. Res.* **1999**, *25*, 65.
10. Olas, B.; Wachowicz, B.; Stochmal, A.; Oleszek, W. *Platelets* **2002**, *13*, 167.
11. Wu, J. M.; Wang, Z. R.; Hsieh, T. C.; Bruder, K. L.; Zou, J. G.; Huang, Y. Z. *Int. J. Mol. Med.* **2001**, *8*, 3.
12. Jang, M.; Cai, L.; Udeani, G. O.; Slowing, K. V.; Thomas, C. F.; Beecher, C. W.; Fong, H. H.; Farnsworth, N. R.; Kinghorn, A. D.; Mehta, R. G.; Moon, R. C.; Pezzuto, J. M. *Science* **1997**, *275*, 218.
13. Jang, M.; Pezzuto, J. M. *Drug Exp. Clin. Res.* **1999**, *25*, 65.
14. Mgbonyebi, O. P.; Russo, J.; Russo, I. H. *Int. J. Oncol.* **1998**, *12*, 865.
15. Uenobe, F.; Nakamura, S.; Miyazawa, M. *Mutat. Res.* **1997**, *373*, 197.
16. Kim, H. J.; Chang, E. J.; Bae, S. J.; Shim, S. M.; Park, H. D.; Rhee, C. H.; Park, J. H.; Choi, S. W. *Arch. Pharm. Res.* **2002**, *25*, 293.
17. Lindenberg, B. A.; Massin, M. J. *J. Physiol. (Paris)* **1957**, *49*, 285.
18. Scannell, R. T.; Barr, J. R.; Murty, V. S.; Reddy, K. S.; Hecht, S. M. *J. Am. Chem. Soc.* **1988**, *110*, 3650.
19. Fukuhara, K.; Miyata, N. *Bioorg. Med. Chem. Lett.* **1998**, *8*, 3187.
20. Sotomatsu, A.; Nakano, M.; Hirai, S. *Arch. Biochem. Biophys.* **1990**, *283*, 334.
21. Seike, K.; Murata, M.; Oikawa, S.; Hiraku, Y.; Hirakawa, K.; Kawanishi, S. *Chem. Res. Toxicol.* **2003**, *16*, 1470.
22. Wang, M.; Jin, Y.; Ho, C.-T. *J. Agric. Food Chem.* **1999**, *47*, 3974.
23. Matsuoka, A.; Takeshita, K.; Furuta, A.; Ozaki, M.; Fukuhara, K.; Miyata, N. *Mutat. Res.* **2002**, *521*, 29.
24. Thakkar, K.; Geahlen, R. L.; Cushman, M. *J. Med. Chem.* **1993**, *36*, 2950.
25. Itoh, S.; Taniguchi, M.; Takada, N.; Nagatomo, S.; Kitagawa, T.; Fukuzumi, S. *J. Am. Chem. Soc.* **2000**, *122*, 12087.
26. Barcelo, F.; Barcelo, I.; Gavilanes, F.; Ferragut, J. A.; Yanovich, S.; Gonzalez-Ros, J. M. *Biochim. Biophys. Acta* **1986**, *884*, 172.

## Regular Article

# *Chenodeoxycholic Acid-mediated Activation of the Farnesoid X Receptor Negatively Regulates Hydroxysteroid Sulfotransferase*

Masaaki MIYATA<sup>1,\*</sup>, Yoshiki MATSUDA<sup>1</sup>, Hiroyuki TSUCHIYA<sup>1</sup>, Hirotaka KITADA<sup>1</sup>,  
Takanori AKASE<sup>1</sup>, Miki SHIMADA<sup>1</sup>, Kiyoshi NAGATA<sup>1</sup>,  
Frank J. GONZALEZ<sup>2</sup> and Yasushi YAMAZOE<sup>1,3</sup>

<sup>1</sup>*Division of Drug Metabolism and Molecular Toxicology, Graduate School of Pharmaceutical Sciences, Tohoku University, Sendai, Japan*

<sup>2</sup>*Laboratory of Metabolism, National Cancer Institute, National Institutes of Health, Bethesda, MD, USA*

<sup>3</sup>*CRESCENDO, The Tohoku University 21<sup>st</sup> Century "Center of Excellence" Program, Sendai, Japan*

Full text of this paper is available at <http://www.jstage.jst.go.jp/browse/dmpk>

**Summary:** Hydroxysteroid sulfotransferase catalyzing bile acid sulfation plays an essential role in protection against lithocholic acid (LCA)-induced liver toxicity. Hepatic levels of Sult2a is up to 8-fold higher in farnesoid X receptor-null mice than in the wild-type mice. Thus, the influence of FXR ligand (chenodeoxycholic acid (CDCA) and LCA) feeding on hepatic Sult2a expression was examined in FXR-null and wild-type mice. Hepatic Sult2a protein content was elevated in FXR-null and wild-type mice fed a LCA (1% and 0.5%) diet. Treatment with 0.5% CDCA diet decreased hepatic Sult2a to 20% of the control in wild-type mice, but increased the content in FXR-null mice. Liver Sult2a1 (St2a4) mRNA levels were reduced to 26% in wild-type mice after feeding of a CDCA diet, while no decrease was observed on Sult2a1 mRNA levels in FXR-null mice after CDCA feeding. A significant inverse relationship ( $r^2 = 0.523$ ) was found between hepatic Sult2a protein content and small heterodimer partner (SHP) mRNA level. PCN-mediated increase in Sult2a protein levels were attenuated by CDCA feeding in wild-type mice, but not in FXR-null mice. Human SULT2A1 protein and mRNA levels were decreased in HepG2 cells treated with the FXR agonists, CDCA or GW4064 in dose-dependent manners, although SHP mRNA levels were increased. These results suggest that SULT2A is negatively regulated through CDCA-mediated FXR activation in mice and humans.

**Key words:** hydroxysteroid sulfotransferase; FXR; bile acid; sulfation; negative regulation; Sult2a

### Introduction

Sulfotransferases (SULT) are phase II metabolizing enzymes that catalyzes sulfation of various endogenous and exogenous chemicals.<sup>1,2)</sup> Hydroxysteroid sulfotransferase (SULT2A) is a cytosolic enzyme expressed abundantly in enterohepatic tissues such as liver and intestine, and also in steroidogenic tissue such as the adrenal cortex.<sup>3)</sup> SULT2A catalyzes the sulfation of drugs, environmental chemicals and endogenous steroids such as dehydroepiandrosterone (DHEA), estrogen and bile acids.<sup>4,5)</sup> SULT2A-mediated sulfation increases the hydrophilicity of bile acids and facilitates their clearance from the body. Because bile acid sulfation

is a main metabolic pathway for bile acid excretion, SULT2A is a critical enzyme for bile acid homeostasis. About 95% of bile acids excreted in bile are reabsorbed in the intestine and thus changes in the level of hepatic SULT2A can disrupt bile acid homeostasis in enterohepatic tissues. SULT2A is also considered to play a major role in the protection against toxic bile acid-induced liver injury in enterohepatic tissues. SULT2A preferably catalyzes the sulfation of hydrophobic and toxic bile acids such as LCA. A protective role of Sult2a against LCA-induced hepatotoxicity was demonstrated by using farnesoid X receptor (FXR)-null female mice constitutively expressing higher levels of Sult2a protein.<sup>6)</sup> The increase in the production of hepatic Sult2a-

Received; February 13, 2006, Accepted; April 7, 2006

\*To whom correspondence should be addressed: Masaaki MIYATA, Ph.D., Division of Drug Metabolism and Molecular Toxicology, Graduate School of Pharmaceutical Sciences, Tohoku University, 6-3, Aoba, Aramaki, Aoba-ku, Sendai, 980-8578, Japan. Tel. +81-22-795-6829, Fax. +81-22-795-6826, E-mail: [miyata@mail.pharm.tohoku.ac.jp](mailto:miyata@mail.pharm.tohoku.ac.jp)

mediated 3 $\alpha$ -sulfated TLCA and the efficient fecal excretion contributes to the protection against LCA-induced toxicity (submitted for publication).

Two Sult2a mRNAs (Sult2a1 (St2a4) and Sult2a2 (St2a9)) that share high homology, were isolated from mice<sup>7,8)</sup> and one mRNA (SULT2A1) has been isolated from humans.<sup>5,9,10)</sup> Mouse Sult2a enzymes are expressed to higher extents in the female. Because of the efficient bile acid sulfating activity in female mice as well as humans, female mice represent a feasible model for bile acid sulfation in humans.

FXR, a member of the nuclear receptor superfamily, is expressed abundantly in liver, intestine and adrenal.<sup>11)</sup> The involvement of FXR in bile acid and lipid homeostasis was demonstrated by using FXR-null mice.<sup>12)</sup> FXR is activated by several bile acids such as CDCA.<sup>13-15)</sup> FXR regulates a variety of genes involved in the metabolism and transport of the lipids such as bile acid and cholesterol. FXR stimulates the expression of Bsep, small heterodimer partner (SHP) and Mrp2, whereas FXR directly represses the expression of apolipoprotein A-I and apolipoprotein C-III, and indirectly suppresses the expression of CYP7A1 and Ntcp through the induction of SHP.<sup>16-18)</sup>

CDCA activation of FXR has been shown to stimulate rat SULT2A1 transcription via the FXR response element (IR0) in HepG2 cells.<sup>19)</sup> Furthermore, it was demonstrated that pregnane X receptor (PXR), constitutive androstane receptor (CAR) and vitamin D receptor (VDR) also bind the rat and mouse IR0 elements and enhance the reporter gene activity.<sup>20-23)</sup> The Sult2a expression level, however, was increased in FXR-null and PXR-null female mice as compared with that of wild-type mice.<sup>6)</sup>

In the present study, SULT2A expression levels were determined using FXR-null mice and HepG2 cells to clarify the involvement of FXR signaling in the suppression of SULT2A gene expression. These results suggest that SULT2A is negatively regulated by activation of FXR with CDCA.

### Materials and Methods

**Materials:** CDCA, LCA, tauroLCA (TLCA), glycoLCA (GLCA), cholic acid (CA), deoxycholic acid (DCA), ursodeoxycholic acid (UDCA), pregnenolone 16 $\alpha$ -carbonitrile (PCN) and dehydroepiandrosterone (DHEA) were purchased from Sigma-Aldrich Co. (St. Louis, MO). GW4064 was kindly provided by Dr. Timothy M. Willson (GlaxoSmithKline, Research Triangle Park, NC).

**Animal treatment and sample collection:** FXR-null female mice<sup>12)</sup> were housed under standard 12-h light/12-h dark cycle. Prior to the administration of special diets, the mice were fed standard rodent chow (CE-2, Clea Japan) and water ad libitum for acclimation. Age-

matched groups of 8- to 12-week-old animals were used for all experiments. The mice were fed the control diet (CE-2) mixed with 0.5% and 1.0% (w/w) LCA for 9 days or 0.5% CDCA for 5 days. The mice were fed the control diet or the diet mixed with 0.5% (w/w) CDCA for 5 days and injected with PCN (100 mg/kg, ip) for the last 3 days.

**Hepatic bile acid concentration:** Hepatic 3 $\alpha$ -hydroxy bile acid concentrations were estimated by an enzyme-colorimetric method using the Total bile acid-test kit from Wako (Wako Pure Chemicals, Osaka, Japan). Hepatic LCA and CDCA contents were measured by HPLC as previously described.<sup>24)</sup>

**Cell culture:** HepG2 cells were plated in 10 cm culture dishes (Falcon Scientific Co., Oxnard, CA) at  $3 \times 10^6$  cells and cultured in Dulbecco's modified Eagle's medium (DMEM) containing 10% fetal calf serum. The cells were cultured for 24-h and then treated with CDCA, GW4064 or vehicle (DMSO) for 48-h. The cells were cultured in serum-free DMEM during chemical treatment.

**Immunoblot analysis:** Cytosolic proteins (30  $\mu$ g/lane) were loaded onto a 9% polyacrylamide gel, isolated and transferred to nitrocellulose filters. The filter was immunostained with a polyclonal antibody prepared against the purified recombinant rat SULT2A1 protein (1:1000 dilution) that reacts with mouse Sult2a<sup>25)</sup> and a polyclonal antibody against the purified recombinant human SULT2A1 protein<sup>26)</sup> (1:1000 dilution) for human SULT2A1. The stained filters were scanned with an Epsom GT-8700 scanner, and the band intensities measured by use of the NIH image (version 1.59) software (Bethesda, MD).

**Expression and purification of Sult2a proteins:** Mouse Sult2a cDNAs were obtained from wild-type mouse liver by reverse transcription-polymerase chain reaction (RT-PCR). Sult2a cDNA fragments, containing a sequence of the recognition site of enterokinase next to the N-terminal methionine of the native form, were obtained by RT-PCR and ligated into the prokaryotic expression vector, pQE30 (QIAGEN). The plasmid DNA was transformed into *Escherichia coli*, M15 (pREP4). Recombinant Sult2a proteins were expressed and purified from bacterial cytosols by nickel-nitrilotriacetic acid affinity chromatography. The fused portion of recombinant Sult2a proteins was removed to yield native proteins for standard of immunoblot analyses by enterokinase.

**Analysis of mRNA levels:** Total RNAs were prepared from livers and HepG2 cells using the RNA-gents Total RNA Isolation System (Promega, Madison, WI), and RNA concentrations were determined by measuring the absorbance at 260 nm using a spectrophotometer (Beckman DU 640). Messenger RNA levels of differentially expressed genes were analyzed